



Cite this: *Phys. Chem. Chem. Phys.*,
2017, **19**, 735

Atmospheric chemistry of *Z*- and *E*-CF₃CH=CHCF₃†

Freja F. Østerstrøm,^{*a} Simone Thirstrup Andersen,^a Theis I. Sølling,^a
Ole John Nielsen^a and Mads P. Sulbaek Andersen^{*ab}

The atmospheric fates of *Z*- and *E*-CF₃CH=CHCF₃ have been studied, investigating the kinetics and the products of the reactions of the two compounds with Cl atoms, OH radicals, OD radicals, and O₃. FTIR smog chamber experiments measured: $k(\text{Cl} + \text{Z-CF}_3\text{CH=CHCF}_3) = (2.59 \pm 0.47) \times 10^{-11}$, $k(\text{Cl} + \text{E-CF}_3\text{CH=CHCF}_3) = (1.36 \pm 0.27) \times 10^{-11}$, $k(\text{OH} + \text{Z-CF}_3\text{CH=CHCF}_3) = (4.21 \pm 0.62) \times 10^{-13}$, $k(\text{OH} + \text{E-CF}_3\text{CH=CHCF}_3) = (1.72 \pm 0.42) \times 10^{-13}$, $k(\text{OD} + \text{Z-CF}_3\text{CH=CHCF}_3) = (6.94 \pm 1.25) \times 10^{-13}$, $k(\text{OD} + \text{E-CF}_3\text{CH=CHCF}_3) = (5.61 \pm 0.98) \times 10^{-13}$, $k(\text{O}_3 + \text{Z-CF}_3\text{CH=CHCF}_3) = (6.25 \pm 0.70) \times 10^{-22}$, and $k(\text{O}_3 + \text{E-CF}_3\text{CH=CHCF}_3) = (4.14 \pm 0.42) \times 10^{-22}$ cm³ molecule⁻¹ s⁻¹ in 700 Torr of air/N₂/O₂ diluents at 296 ± 2 K. *E*-CF₃CH=CHCF₃ reacts with Cl atoms to give CF₃CHClC(O)CF₃ in a yield indistinguishable from 100%. *Z*-CF₃CH=CHCF₃ reacts with Cl atoms to give (95 ± 10)% CF₃CHClC(O)CF₃ and (7 ± 1)% *E*-CF₃CH=CHCF₃. CF₃CHClC(O)CF₃ reacts with Cl atoms to give the secondary product CF₃C(O)Cl in a yield indistinguishable from 100%, with the observed co-products C(O)F₂ and CF₃O₃CF₃. The main atmospheric fate for *Z*- and *E*-CF₃CH=CHCF₃ is reaction with OH radicals. The atmospheric lifetimes of *Z*- and *E*-CF₃CH=CHCF₃ are estimated as 27 and 67 days, respectively. IR absorption cross sections are reported and the global warming potentials (GWPs) of *Z*- and *E*-CF₃CH=CHCF₃ for the 100 year time horizon are calculated to be GWP₁₀₀ = 2 and 7, respectively. This study provides a comprehensive description of the atmospheric fate and impact of *Z*- and *E*-CF₃CH=CHCF₃.

Received 21st October 2016,
Accepted 27th November 2016

DOI: 10.1039/c6cp07234h

www.rsc.org/pccp

1. Introduction

Chlorofluorocarbons (CFCs) are well-known for their ability to destroy stratospheric ozone and their potency as greenhouse gases.^{1–3} They have had several uses, for instance as refrigerants, solvents, in foam blowing and in electronic cleaning.⁴ Having recognized their environmental and atmospheric impacts they were phased out and replaced by hydrochlorofluorocarbons (HCFCs) and hydrofluorocarbons (HFCs). Generally, the HCFCs and HFCs are more environmentally benign in that the HCFCs and HFCs have shorter atmospheric lifetimes than the CFCs, and that the HFCs do not contain chlorine substituents. However, they are both still long-lived greenhouse gases.

Hydrofluoroolefins (HFOs) constitutes a recent class of alternative replacement compounds to the CFCs, HCFCs, and HFCs. They are more reactive in the atmosphere and thereby have a smaller impact on the environment. It is important to know the fate of these compounds before they enter large-scale

production and are potentially released to the environment. *Z*- and *E*-CF₃CH=CHCF₃ (1,1,1,4,4,4-hexafluoro-2-butene, HFO-1336mzzm) belong to this class of proposed HFOs. CF₃CH=CHCF₃ has been proposed to be used for foam blowing with an improvement of the energy efficiency of the process and the *Z*-isomer has been shown to have beneficial properties as a substitute for CF₃CH₂CHF₂ (1,1,1,3,3-pentafluoropropane, HFC-245fa) as a refrigerant in organic Rankine cycles.^{5,6} The photochemical reactor setup at the Copenhagen Center for Atmospheric Research (CCAR) was used to study the atmospheric chemistry of the *Z*- and *E*-isomers of CF₃CH=CHCF₃. The reactions of the two isomers with Cl atoms, OH radicals, OD radicals, and O₃ were studied, investigating the kinetics and the products of the reactions with Cl atoms in order to assess the fates of the compounds in the atmosphere. Only one previous study of the *Z*-isomer by Baasandorj *et al.*⁷ exists in the literature. OH radicals, and to a lesser degree, Cl atoms, and O₃ are atmospheric oxidants that initiates the atmospheric removal of *Z*- and *E*-CF₃CH=CHCF₃. The kinetics of the reaction of *Z*-CF₃CH=CHCF₃ with OD radicals was also investigated in the aforementioned study by Baasandorj *et al.*, so OD radical experiments have been included here to be able to compare the present study to their work.⁷ We present here the first determination of the Cl atom and O₃ initiated chemistry of *Z*-CF₃CH=CHCF₃ and the first determination of the atmospheric

^a Department of Chemistry, Copenhagen Center for Atmospheric Research, University of Copenhagen, Universitetsparken 5, DK-2100 Copenhagen Ø, Denmark. E-mail: freja.oesterstroem@gmail.com

^b Department of Chemistry and Biochemistry, California State University Northridge, 18111 Nordhoff St., Northridge, CA 91330-8262, USA. E-mail: mpsa@csun.edu

† Electronic supplementary information (ESI) available. See DOI: 10.1039/c6cp07234h

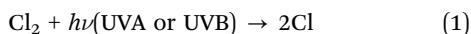


chemistry of $E\text{-CF}_3\text{CH}=\text{CHCF}_3$. The findings from the present study are discussed with respect to the atmospheric chemistry of HFOs.

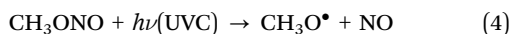
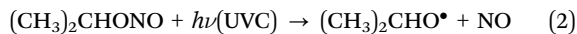
2. Methodology

2.1 Experimental methods

The CCAR photoreactor is a 101.4 L quartz reactor surrounded by 8 UVA (Osram Eversun L100/79 with the main emission peak at 368 nm) or UVB (Waldmann F85/100 UV6, with a wavelength range of 280–360 nm) lamps, and 16 UVC lamps that are used to initiate the experiments. The reactor is interfaced with a Bruker IFS 66 v/s FTIR spectrometer.⁸ All spectra were obtained using 32 co-added interferograms with a spectral resolution of 0.25 cm^{-1} and optical pathlengths of 45.10, 52.67, and 55.55 meters. All experiments were performed at $296 \pm 2\text{ K}$ and at a total pressure of 700 Torr air/ N_2/O_2 diluent. The experiments were performed with Cl atoms, OH radicals, OD radicals or O_3 . Cl atoms were produced by photolysis of Cl_2 :



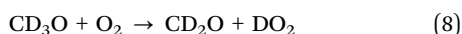
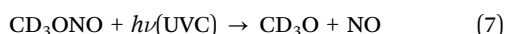
OH radicals were produced by the photolysis of $(\text{CH}_3)_2\text{CHONO}$ (isopropyl nitrite) or CH_3ONO (methyl nitrite) followed by reaction with O_2 forming HO_2 :



The HO_2 formed from $(\text{CH}_3)_2\text{CHONO}$ or CH_3ONO reacts with NO to give OH radicals:

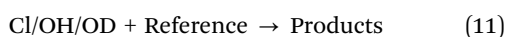
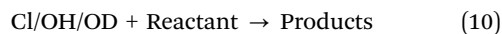


OD radicals were produced by photolysis of CD_3ONO (deuterated methyl nitrite):



O_3 was produced using a commercial ozone generator from O_3 -Technology (Dielectric barrier discharge; model AC-20). The O_3 was pre-concentrated on a silica gel trap to reduce the amount of O_2 introduced to the chamber.

The relative rate method is a well-known method for measuring rate coefficients of gas phase reactions. The reactions of the reactants (Z - and $E\text{-CF}_3\text{CH}=\text{CHCF}_3$) with the oxidants are measured relative to the reactions of reference compounds with the oxidants:



Plotting the loss of reactant *versus* the loss of reference the following equation is used:

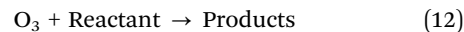
$$\ln\left(\frac{[\text{Reactant}]_{t_0}}{[\text{Reactant}]_t}\right) = \frac{k_{\text{Reactant}}}{k_{\text{Reference}}} \ln\left(\frac{[\text{Reference}]_{t_0}}{[\text{Reference}]_t}\right) \quad (I)$$

where $[\text{Reactant}]_{t_0}$, $[\text{Reactant}]_t$, $[\text{Reference}]_{t_0}$ and $[\text{Reference}]_t$ are the concentrations of the reactant and the reference at times t_0 and t . k_{Reactant} and $k_{\text{Reference}}$ are the rate coefficients of the reactant and the reference reactions, respectively. The slope of the fit of the experimental data to eqn (I) provides the rate coefficient ratio $k_{\text{Reactant}}/k_{\text{Reference}}$. For the experiments with Cl atoms C_2H_2 , C_2H_4 , C_2H_6 , and $\text{CH}_3\text{C}(\text{O})\text{CH}_3$ were used as references. For the experiments with OH radicals C_3H_8 and C_2H_6 were used as references. For the experiments with OD radicals C_2H_6 and $n\text{-C}_4\text{H}_{10}$ were used as references.

An absolute rate method was used in the O_3 kinetic experiments. Here the loss of the reactant is monitored over time with an excess of O_3 :

$$\ln\left(\frac{[\text{Reactant}]_t}{[\text{Reactant}]_{t_0}}\right) = -k^{\text{pseudo 1st}} \times t = -k_{12} \times [\text{O}_3] \times t \quad (II)$$

The pseudo first order rate coefficients ($k^{\text{pseudo 1st}}$) obtained from the individual experiments are plotted against the varying O_3 concentrations giving the rate coefficient k_{12} of the reaction as the slope of the line fitted to the data:



All reagents except CD_3ONO , CH_3ONO , and $(\text{CH}_3)_2\text{CHONO}$ were obtained from commercial sources. Z - and $E\text{-CF}_3\text{CH}=\text{CHCF}_3$ were produced by SynQuest Laboratories at quoted purities of $\leq 100\%$. $Z\text{-CF}_3\text{CH}=\text{CHCF}_3$ was supplied to us by Honeywell. Ultrapure N_2 ($\geq 99.999\%$), ultrapure O_2 ($\geq 99.995\%$), synthetic air, $Z\text{-CF}_3\text{CH}=\text{CHCF}_3$, and $E\text{-CF}_3\text{CH}=\text{CHCF}_3$ were used as received. The $Z\text{-CF}_3\text{CH}=\text{CHCF}_3$ sample was devoid of any impurities as analyzed by FTIR. The sample of $E\text{-CF}_3\text{CH}=\text{CHCF}_3$ contained an impurity of 1.8% $Z\text{-CF}_3\text{CH}=\text{CHCF}_3$, which was taken into account in the analysis of the IR spectra. CD_3ONO , CH_3ONO , and $(\text{CH}_3)_2\text{CHONO}$ were produced by the dropwise addition of cold H_2SO_4 (sulfuric acid) to a mixture of NaNO_2 (sodium nitrite) and CD_3OH (deuterated methanol), CH_3OH (methanol) or $(\text{CH}_3)_2\text{CHOH}$ (isopropanol), respectively. The produced nitrites were trapped using either an ice bath or an isopropanol/dry ice bath. They were stored cold and in the dark. CD_3ONO , CH_3ONO , and $(\text{CH}_3)_2\text{CHONO}$ were subjected to freeze–pump–thaw cycling before use. The CD_3ONO , CH_3ONO , and $(\text{CH}_3)_2\text{CHONO}$ samples were devoid of impurities as analyzed by FTIR.

To test for unwanted loss of reagents due to photolysis, dark reactions and heterogeneous reactions, control experiments were performed to investigate these processes. Samples of Z - and $E\text{-CF}_3\text{CH}=\text{CHCF}_3$ in the chamber were irradiated with UV with no observable loss. Reactant/product mixtures obtained after UV irradiation were allowed to stand in the dark for 30 minutes. No loss or changes were observed, indicating that loss processes due to dark reactions or heterogeneous reactions are not a complication in these experiments. Unless otherwise stated,



the quoted uncertainties are two standard deviations from the least-squares fits and our estimated uncertainty of the analysis (typically $\pm 1\%$ of initial concentrations).

2.2 Computational methods

The calculations were carried out with a fourth generation composite method referred to as G4MP2⁹ with the GAUSSIAN 09, suite of programs.¹⁰ G4MP2 theory is approximating a large basis set CCSD(T) single point calculation on a B3LYP/6-31G(2df,p) geometry and is incorporating a so-called higher level correction that is derived by a fit to the experimental values in the G3/05 test set with 454 experimental values.¹¹ The average absolute derivation from the experimental test set values is $1.04 \text{ kcal mol}^{-1}$, which places the G4MP2 results well within chemical accuracy of 10 kJ mol^{-1} . The transition structures for the reactions reported in this work have been confirmed in each case by the calculation of vibrational frequencies (one imaginary frequency) and an intrinsic reaction coordinate analysis. Relative free energies stated within the text correspond to G4MP2 values at 298.15 K. The calculated total energies are available as ESI† (Table S1), which also includes the B3LYP/6-31G(2df,p) optimized geometries in the form of GAUSSIAN archive entries (Table S2, ESI†).

The energies of deuterated species were evaluated using the Freq=readiso keyword with an input from the B3LYP/6-31G(2df,p) frequency calculations. The frequencies were also scaled by 0.9854 as for the G4MP2 calculations. The free energy contributions were obtained in this manner together with the relevant partition functions for the evaluation of relative rate coefficients.

Calculations of theoretical IR spectra used in the product studies were performed with the GAUSSIAN 09, suite of programs,¹² using B3LYP/6-31+G(d,p) and ω B97XD/cc-pVTZ frequency calculations. Optimized geometries and IR spectra can be found in the ESI† (Tables S3–S11 and Fig. S1–S9).

3. Results and discussion

3.1 Relative rate study of Z- and E-CF₃CH=CHCF₃ + Cl

The rates of reactions (13) and (14) were measured relative to reactions (15–17) and (15), (17), and (18), respectively. The initial reaction mixtures were 1.56–2.61 mTorr Z- or E-CF₃CH=CHCF₃, 72.1–83.3 mTorr Cl₂, and 10.4–10.5 mTorr C₂H₂, 5.21 mTorr C₂H₄, 7.82 mTorr C₂H₆ or 10.0–10.4 mTorr CH₃C(O)CH₃ in 700 Torr air. The mixtures were subjected to a total of 25–76 seconds of UV irradiation.

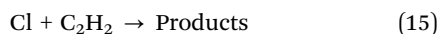


Fig. 1 shows the loss of Z- and E-CF₃CH=CHCF₃ versus the loss of the reference compounds. Linear least squares analyses of

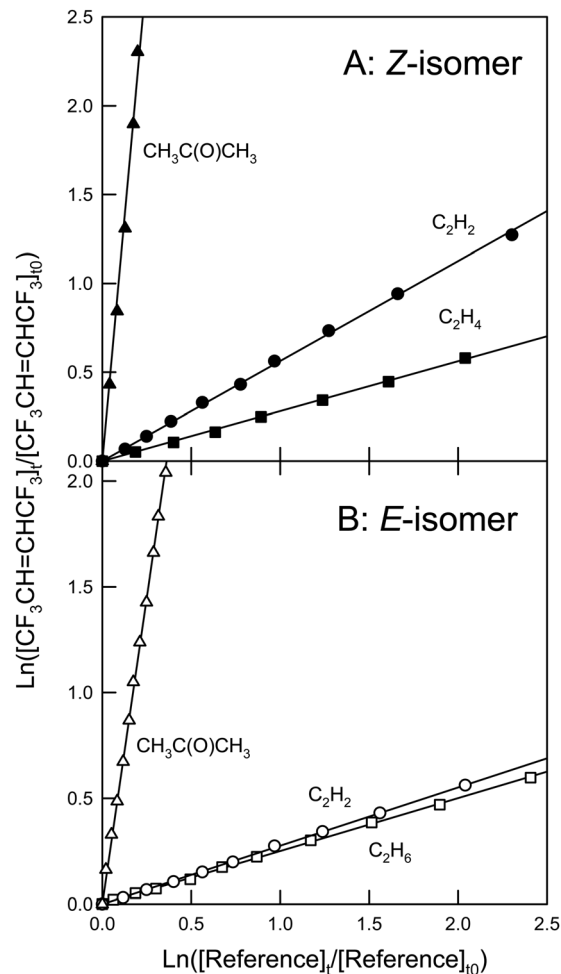


Fig. 1 Panel A: Loss of Z-CF₃CH=CHCF₃ versus the loss of C₂H₂ (circles), C₂H₄ (squares), and CH₃C(O)CH₃ (triangles) in the presence of Cl atoms. Panel B: Loss of E-CF₃CH=CHCF₃ versus the loss of C₂H₂ (circles), C₂H₆ (squares), and CH₃C(O)CH₃ (triangles) in the presence of Cl atoms.

the data for k_{13} in Fig. 1 gives the rate coefficient ratios $k_{13}/k_{15} = 0.56 \pm 0.06$, $k_{13}/k_{16} = 0.28 \pm 0.03$, and $k_{13}/k_{17} = 11.0 \pm 1.21$. Using $k_{15} = (5.07 \pm 0.34) \times 10^{-11}$,¹³ $k_{16} = (9.29 \pm 0.51) \times 10^{-11}$,¹³ and $k_{17} = (2.10 \pm 0.15) \times 10^{-12}$ ¹⁴ gives $k_{13} = (2.85 \pm 0.29) \times 10^{-11}$, $(2.61 \pm 0.26) \times 10^{-11}$, and $(2.31 \pm 0.25) \times 10^{-11} \text{ cm}^3 \text{ molecule}^{-1} \text{ s}^{-1}$, respectively. The values for k_{13} are identical within the ranges of uncertainty. Using a similar approach three rate coefficient values for k_{14} were obtained. A summary of all the rate coefficient ratios and individual rate coefficient determinations in this work is shown in Table 1. The three values for k_{14} are also identical within the ranges of uncertainty (see Table 1). We choose to quote final values for k_{13} and k_{14} as the averages of the three determinations with uncertainties that encompass the extremes of the individual determinations. Hence, $k_{13} = (2.59 \pm 0.47) \times 10^{-11}$ and $k_{14} = (1.36 \pm 0.27) \times 10^{-11} \text{ cm}^3 \text{ molecule}^{-1} \text{ s}^{-1}$.

This is the first determination of k_{13} and k_{14} . The value of k_{14} is approximately half of k_{13} . The magnitudes of k_{13} and k_{14} are consistent with expectations based on the reactivities of similar HFOs such as E-CF₃CH=CHF, Z- and E-CF₃CF=CHF, and CF₃CF=CF₂, which have the rate coefficient values



Table 1 Rate coefficient ratios, reference rate coefficient values, and the individual determinations of the rate coefficients of the reactions of *Z*-CF₃CH=CHCF₃ (*Z*) and *E*-CF₃CH=CHCF₃ (*E*) with Cl atoms, OH radicals, and OD radicals

Reaction	Reference	$k_{\text{Reactant}}/k_{\text{Reference}}$	$k_{\text{Reference}}$ (cm ³ molecule ⁻¹ s ⁻¹)	k_{Reactant} (cm ³ molecule ⁻¹ s ⁻¹)
Z + Cl	C ₂ H ₂	0.56 ± 0.06	(5.07 ± 0.34) × 10 ^{-11 a}	(2.85 ± 0.29) × 10 ⁻¹¹
Z + Cl	C ₂ H ₄	0.28 ± 0.03	(9.29 ± 0.51) × 10 ^{-11 a}	(2.61 ± 0.26) × 10 ⁻¹¹
Z + Cl	CH ₃ C(O)CH ₃	11.0 ± 1.21	(2.1 ± 0.15) × 10 ^{-12 b}	(2.31 ± 0.25) × 10 ⁻¹¹
Z + OH	C ₃ H ₈	0.38 ± 0.06	(1.1 ± 0.08) × 10 ^{-12 b}	(4.14 ± 0.40) × 10 ⁻¹³
Z + OH	C ₂ H ₆	1.78 ± 0.18	(2.4 ± 0.08) × 10 ^{-13 b}	(4.27 ± 0.44) × 10 ⁻¹³
Z + OD	C ₂ H ₆	2.70 ± 0.29	(2.74 ± 0.27) × 10 ^{-13 c}	(7.39 ± 0.80) × 10 ⁻¹³
Z + OD	<i>n</i> -C ₄ H ₁₀	0.23 ± 0.03	(2.76 ± 0.22) × 10 ^{-12 d}	(6.49 ± 0.75) × 10 ⁻¹³
<i>E</i> + Cl	C ₂ H ₂	0.28 ± 0.03	(5.07 ± 0.34) × 10 ^{-11 a}	(1.40 ± 0.14) × 10 ⁻¹¹
<i>E</i> + Cl	C ₂ H ₆	0.25 ± 0.03	(5.9 ± 0.06) × 10 ^{-11 b}	(1.48 ± 0.15) × 10 ⁻¹¹
<i>E</i> + Cl	CH ₃ C(O)CH ₃	5.80 ± 0.58	(2.1 ± 0.15) × 10 ^{-12 b}	(1.22 ± 0.12) × 10 ⁻¹¹
<i>E</i> + OH	C ₃ H ₈	0.14 ± 0.02	(1.1 ± 0.08) × 10 ^{-12 b}	(1.52 ± 0.19) × 10 ⁻¹³
<i>E</i> + OH	C ₂ H ₆	0.80 ± 0.10	(2.4 ± 0.08) × 10 ^{-13 b}	(1.91 ± 0.23) × 10 ⁻¹³
<i>E</i> + OD	C ₂ H ₆	2.05 ± 0.26	(2.74 ± 0.27) × 10 ^{-13 c}	(5.63 ± 0.71) × 10 ⁻¹³
<i>E</i> + OD	<i>n</i> -C ₄ H ₁₀	0.20 ± 0.02	(2.76 ± 0.22) × 10 ^{-12 d}	(5.59 ± 0.68) × 10 ⁻¹³

^a Wallington *et al.*¹³ ^b Atkinson *et al.*¹⁴ ^c Grenier.³⁶ ^d Paraskevopoulos and Nip.³⁷

(4.64 ± 0.59) × 10⁻¹¹,¹⁵ (4.36 ± 0.48) × 10⁻¹¹,¹⁶ (5.00 ± 0.56) × 10⁻¹¹,¹⁶ and (2.7 ± 0.3) × 10⁻¹¹¹⁷ cm³ molecule⁻¹ s⁻¹, respectively.

3.2 Relative rate study of *Z*- and *E*-CF₃CH=CHCF₃ + OH

The rate of reaction (19) and (20) were measured relative to reactions (21) and (22). The reaction mixtures consisted of 1.60–1.98 mTorr *Z*-CF₃CH=CHCF₃ or 2.08 mTorr *E*-CF₃CH=CHCF₃, 7.19–7.40 mTorr C₃H₈ or 7.30 mTorr C₂H₆, and 73.0 mTorr (CH₃)₂CHONO or 157–224 mTorr CH₃ONO in 700 Torr of air. The mixtures were subjected to a total of 265–3180 seconds of UV irradiation.

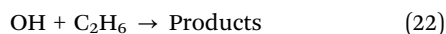
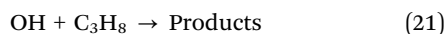
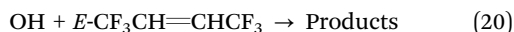
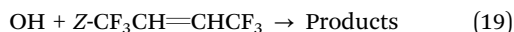


Fig. 2 shows the loss of *Z*- and *E*-CF₃CH=CHCF₃ versus the loss of reference compounds C₃H₈ and C₂H₆ in the presence of OH radicals. Rate coefficient ratios obtained from linear least squares analyses of the data in Fig. 2 are shown in Table 1. Using the rate coefficient values of $k_{21} = (1.1 \pm 0.08) \times 10^{-12}$ and $k_{22} = (2.4 \pm 0.08) \times 10^{-13}$ cm³ molecule⁻¹ s⁻¹,¹⁴ gives two values for each k_{19} and k_{20} , which are identical within the ranges of uncertainty (Table 1). We choose to quote final values for k_{19} and k_{20} as the average of the two determinations with uncertainties that encompass the extremes of the individual determinations. Hence, $k_{19} = (4.21 \pm 0.62) \times 10^{-13}$ and $k_{20} = (1.72 \pm 0.42) \times 10^{-13}$ cm³ molecule⁻¹ s⁻¹. Baasandorj *et al.*⁷ reported a value for k_{19} of $(4.91 \pm 0.50) \times 10^{-13}$ cm³ molecule⁻¹ s⁻¹, which is in reasonable agreement with the value determined here. The value of k_{20} is approximately 2/5 the size of k_{19} . The values for k_{19} and k_{20} determined in the present work are consistent with expectations based on the OH radical reactivities of similar HFOs such as *Z*- and *E*-CF₃CF=CHF and *Z*- and *E*-CF₃CH=CHCl, which have rate coefficients of

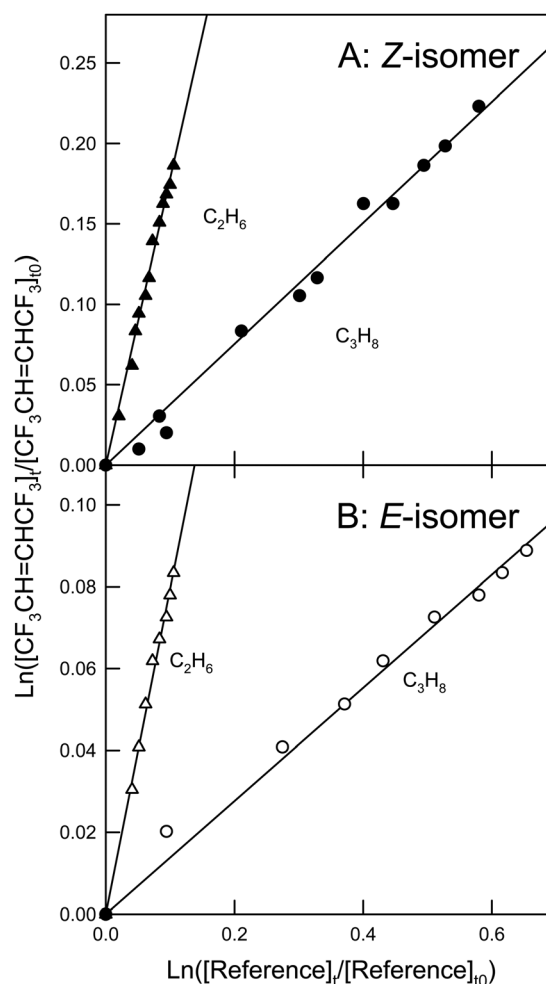


Fig. 2 Panel A: Loss of *Z*-CF₃CH=CHCF₃ versus the loss of C₃H₈ (circles) and C₂H₆ (triangles) in the presence of OH radicals. Panel B: Loss of *E*-CF₃CH=CHCF₃ versus the loss of C₃H₈ (circles) and C₂H₆ (triangles) in the presence of OH radicals.

(1.22 ± 0.14) × 10⁻¹²,¹⁶ (2.15 ± 0.23) × 10⁻¹²,¹⁶ (8.45 ± 1.52) × 10⁻¹³,¹⁸ and (3.61 ± 0.37) × 10⁻¹³ cm³ molecule⁻¹ s⁻¹,¹⁸ respectively.



3.3 Relative rate study of *Z*- and *E*-CF₃CH=CHCF₃ + OD

The rate of reactions (23) and (24) were measured relative to reactions (25) and (26). The initial reaction mixtures consisted of 1.68–2.08 mTorr *Z*- or *E*-CF₃CH=CHCF₃, 6.67–8.34 mTorr C₂H₆ or 7.30–8.24 mTorr *n*-C₄H₁₀, and 169–230.4 mTorr CD₃ONO in 700 Torr air. The mixtures were subject to a total of 860–1080 seconds of UV irradiation.

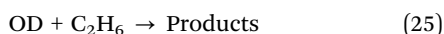
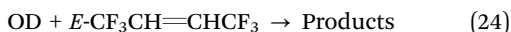
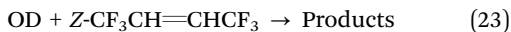


Fig. 3 shows the loss of *Z*- and *E*-CF₃CH=CHCF₃ versus the loss of the two reference compounds C₂H₆ and *n*-C₄H₁₀ in the presence of OD radicals. Linear regression of the data gives the rate coefficient ratios and values of *k*₂₃ and *k*₂₄ shown in Table 1. The two values for *k*₂₃ are identical within the ranges of uncertainty. The same is the case for *k*₂₄. We choose to quote

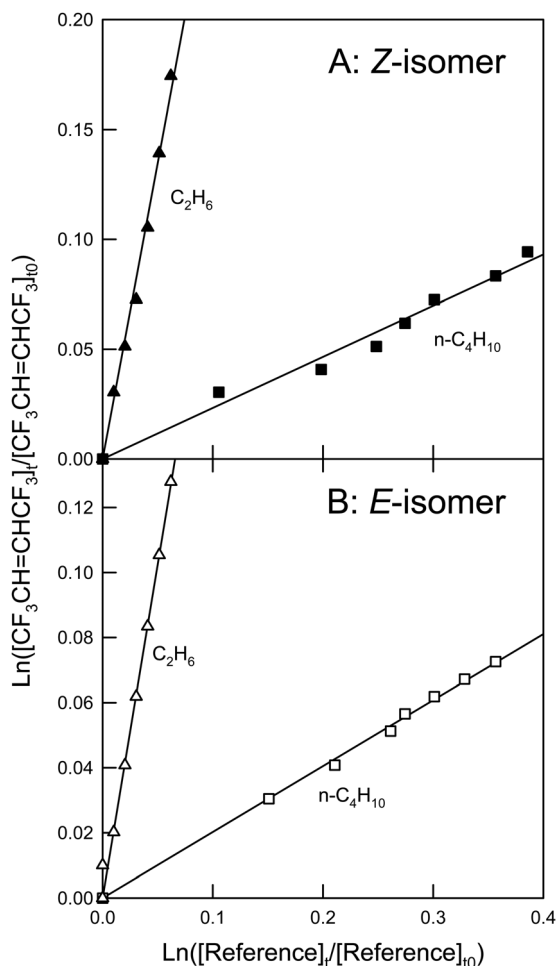


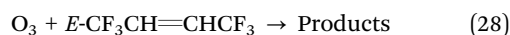
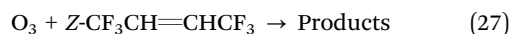
Fig. 3 Panel A: Loss of *Z*-CF₃CH=CHCF₃ versus the loss of C₂H₆ (circles) and *n*-C₄H₁₀ (squares) in the presence of OD radicals. Panel B: Loss of *E*-CF₃CH=CHCF₃ versus the loss of C₂H₆ (circles) and *n*-C₄H₁₀ (squares) in the presence of OD radicals.

final values for *k*₂₃ and *k*₂₄ as the averages of the two determinations with uncertainties that encompass the extremes of the individual determinations. Hence, *k*₂₃ = (6.94 ± 1.25) × 10⁻¹³ and *k*₂₄ = (5.61 ± 0.98) × 10⁻¹³ cm³ molecule⁻¹ s⁻¹. The value of *k*₂₃ determined here is slightly higher than that reported by Baasandorj *et al.* ((5.73 ± 0.50) × 10⁻¹³ cm³ molecule⁻¹ s^{-1.7}), still they are in agreement within the ranges of uncertainty.

No other studies of OD radicals with HFOs are available in the literature making it difficult to compare the values of *k*₂₃ and *k*₂₄ to other similar compounds. The value of *k*₂₄ is 4/5 the size of *k*₂₃. This was unexpected, since the reactions of *E*-CF₃CH=CHCF₃ with the other oxidants in this study are significantly lower than the corresponding reactions of *Z*-CF₃CH=CHCF₃.

3.4 Absolute rate study of *Z*- and *E*-CF₃CH=CHCF₃ + O₃

Reaction mixtures consisted of 1.53–1.78 mTorr *Z*-CF₃CH=CHCF₃ or 2.08–2.81 mTorr *E*-CF₃CH=CHCF₃, 0.73–6.41 Torr O₃, and 0–10.4 mTorr *c*-C₆H₁₂ (cyclohexane) in 700 Torr air or 140 Torr O₂ made up to 700 Torr with N₂. Reaction (27) and (28) were monitored over time.



Ozonolysis can be a source of OH radicals. To avoid complications due to the reaction of *Z*- and *E*-CF₃CH=CHCF₃ + OH, *c*-C₆H₁₂ was added to the reaction mixture as an OH radical scavenger. In the absence of *c*-C₆H₁₂ the loss of *Z*-CF₃CH=CHCF₃ + O₃ was found to be approximately 15% higher than when *c*-C₆H₁₂ was present. Over the ratios of [*c*-C₆H₁₂]/[*Z*- or *E*-CF₃CH=CHCF₃] = 1.8–6.8 no difference in the O₃ reaction rate was observed. Fig. 4 and Fig. S1 in the ESI† show plots of the pseudo first order rate coefficients for *Z*- and *E*-CF₃CH=CHCF₃ versus O₃ concentration, with the former obtained from the slopes of the degradation of *Z*- and *E*-CF₃CH=CHCF₃ versus time at different O₃ concentrations (see insets in Fig. 4 and Fig. S1, ESI†). The slopes of the plots in Fig. 4 and Fig. S1 (ESI†) give the O₃ rate coefficients for *Z*- and *E*-CF₃CH=CHCF₃, respectively. Hence, *k*₂₇ = (6.25 ± 0.70) × 10⁻²² and *k*₂₈ = (4.14 ± 0.42) × 10⁻²² cm³ molecule⁻¹ s⁻¹.

Baasandorj *et al.*⁷ reported an upper limit for the reaction of *Z*-CF₃CH=CHCF₃ + O₃ of *k*₂₇ < 6 × 10⁻²¹ cm³ molecule⁻¹ s⁻¹, which is in agreement with the rate coefficient determined in the present work. The measured rate coefficient for reaction (28) is the slowest rate coefficient ever determined using the photochemical reactor at CCAR. Prior to this study the slowest rate coefficient for a similar compound reacting with ozone determined is of the reaction of *Z*-CF₃CF=CHF + O₃, which is determined to be (1.45 ± 0.15) × 10⁻²¹ cm³ molecule⁻¹ s^{-1.16}. The value of *k*₂₈ is approximately 2/3 that of *k*₂₇.

3.5 Reactivity trends

As mentioned earlier, one previous study⁷ exists in the literature on the reactivity of *Z*-CF₃CH=CHCF₃, but no studies have ever been conducted involving *E*-CF₃CH=CHCF₃. Furthermore, the kinetic study of Baasandorj *et al.* was limited to the reactions of OH radicals, OD radicals and O₃. The rate coefficients reported



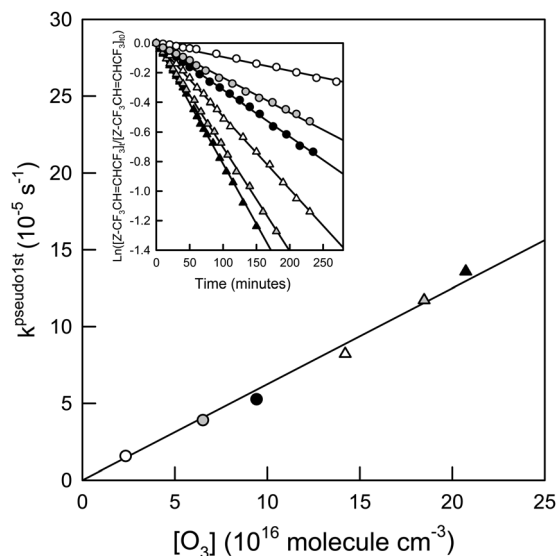


Fig. 4 Pseudo first-order rate coefficients of the reaction $O_3 + Z-CF_3CH=CHCF_3$ versus O_3 concentration. The inset shows the loss of $Z-CF_3CH=CHCF_3$ versus time at different O_3 concentrations. The symbols indicate different O_3 partial pressures: 0.73 Torr (white circles), 2.01 Torr (gray circles), 2.91 Torr (black circles), 4.39 Torr (white triangles), 5.71 Torr (gray triangles), and 6.41 Torr (black triangles). See text for details.

by Baasandorj *et al.*⁷ are all in agreement with our results, although Baasandorj *et al.*⁷ also conclude that $k_{OD} = k_{OH}$ for $Z-CF_3CH=CHCF_3$ within their reported uncertainties. As seen from Table 1, this is contrary to our findings. We find that the rate coefficient for the reaction with OD radicals is larger than that for the reaction with OH radicals for both compounds. Using computational methods, we investigate this further in Section 3.6.

A summary of the final rate coefficients obtained for all the kinetic experiments is shown in Table 2 along with the rate coefficient values determined previously by Baasandorj *et al.* as well as rate coefficients of the reactions for other structurally similar HFOs. The *Z*-isomer has reaction rate coefficients that

are greater than those of the *E*-isomer in the reactions with all the oxidants studied here. This can be explained by the structural differences of the *Z*- and *E*-isomers, where more strain is released from the *Z*-isomer upon addition of the oxidants to the double bond, making it more favorable. Some trends can be observed for the HFOs presented in Table 2. Firstly, the rate coefficients of the reactions with Cl atoms determined here are of the same order as the ones determined for other similar HFOs, but with smaller reaction rate coefficients than the partially fluorinated HFOs, indicating a decrease in reactivity when exchanging a halogen atom (Cl or F) with a CF_3 group. For $CF_3CF=CHF$ and $CF_3CH=CHCl$ the reactivities of the *Z*- and *E*-isomers towards Cl atoms are identical within the ranges of uncertainty. In this study the reactivity of the *Z*-isomer of $CF_3CH=CHCF_3$ has been found to be greater than that of the *E*-isomer. Secondly, the reactions of $CF_3CF=CF_2$, *Z*- and *E*- $CF_3CF=CHF$ with OH radicals proceed with rate coefficients that are one order of magnitude larger than those determined for the other HFOs. This could indicate an increasing effect on the reactivity towards OH radicals by having fluorine on both carbons on the double bond. Additional computational studies could aid the interpretation of this observation. The length of the perfluorinated chain may not be of great importance since the rate coefficient of $E-(CF_3)_2CFCH=CHF + OH$ is approximately half the size of the one of $E-CF_3CH=CHF + OH$ and identical to the one of $E-CF_3CH=CHCl + OH$. Thirdly, the HFOs listed from literature have reactivities towards O_3 that are 1–2 orders of magnitude faster than the O_3 reactivities of *Z*- and *E*- $CF_3CH=CHCF_3$. This could be due to differences in reactivity of fluorinated propenes and butenes towards O_3 . Additional studies on other fluorinated butenes would be needed to verify this.

It is interesting to compare the reactivities of *Z*- and *E*- $CF_3CH=CHCF_3$ to *Z*- and *E*- $CF_3CH=CHCl$. For both pairs of isomers it can be seen in Table 2 that both the Cl atom, the OH radical and the O_3 rate coefficients obtained for the *Z*-isomers are faster than the ones obtained for the *E*-isomers.^{18,19} All the rate coefficients obtained for *Z*- and *E*- $CF_3CH=CHCl$ are larger than for *Z*- and *E*- $CF_3CH=CHCF_3$ even though they have the

Table 2 Final rate coefficients for the reactions of *Z*- and *E*- $CF_3CH=CHCF_3$ with Cl atoms, OH radicals, OD radicals, and O_3 as well as the available literature data for $Z-CF_3CH=CHCF_3$ and structurally similar HFOs. All units are $cm^3 \text{ molecule}^{-1} \text{ s}^{-1}$

Compound	k_{Cl} (10^{-11})	k_{OH} (10^{-13})	k_{OD} (10^{-13})	k_{O_3} (10^{-22})
<i>Z</i> - $CF_3CH=CHCF_3$	2.59 ± 0.47	4.21 ± 0.62	6.94 ± 1.25	6.25 ± 0.70
<i>E</i> - $CF_3CH=CHCF_3$	1.36 ± 0.27	4.91 ± 0.50^a	5.73 ± 0.50^a	$<60^a$
<i>Z</i> - $CF_3CH=CHCl$	6.26 ± 0.84^b	8.45 ± 1.52^b	—	15.3 ± 1.20^b
<i>E</i> - $CF_3CH=CHCl$	5.22 ± 0.72^d	9.46 ± 0.85^c	—	—
	—	3.61 ± 0.37^b	—	14.6 ± 1.20^d
	—	3.76 ± 0.35^c	—	—
<i>Z</i> - $CF_3CF=CHF$	4.36 ± 0.48^e	12.2 ± 1.4^e	—	14.5 ± 1.5^e
<i>E</i> - $CF_3CF=CHF$	5.00 ± 0.56^e	21.5 ± 2.3^e	—	198 ± 15^e
<i>E</i> - $CF_3CH=CHF$	4.64 ± 0.59^f	9.25 ± 1.72^f	—	28.1 ± 2.1^f
$CF_3CF=CF_2$	2.7 ± 0.3^g	24 ± 3^g	—	$<30^g$
<i>E</i> - $(CF_3)_2CFCH=CHF$	—	3.26 ± 0.26^h	—	—

^a Baasandorj *et al.*⁷ ^b Andersen *et al.*¹⁸ ^c Gierczak *et al.*³⁸ ^d Sulbaek Andersen *et al.*¹⁹ ^e Hurley *et al.*¹⁶ ^f Søndergaard *et al.*¹⁵ ^g Mashino *et al.*¹⁷ ^h Papadimitriou and Burkholder.³⁹



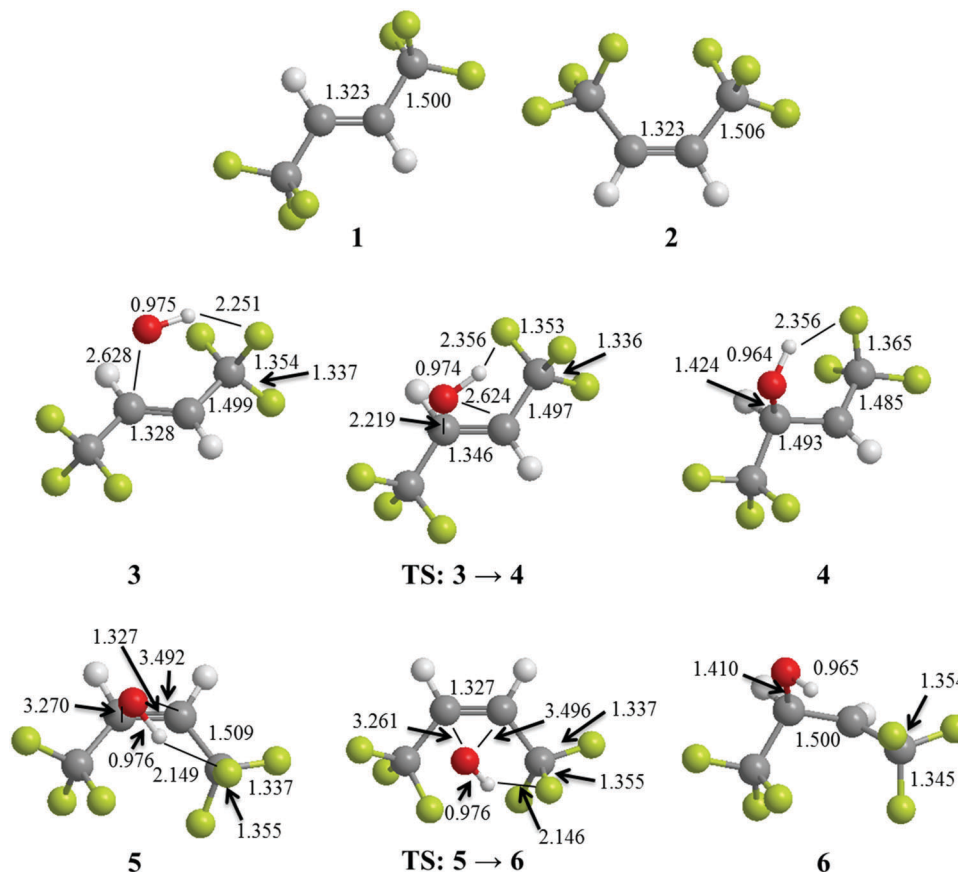


Fig. 5 Structures of optimized geometries of 1: *E*-CF₃CH=CHCF₃, 2: *Z*-CF₃CH=CHCF₃, 3: complex of OH + *E*-CF₃CH=CHCF₃, 4: alkyl radical product formed from OH + *E*-CF₃CH=CHCF₃, 5: complex of OH + *Z*-CF₃CH=CHCF₃, 6: alkyl radical product formed from OH + *Z*-CF₃CH=CHCF₃, and transition states (TS) connecting 3 → 4 and 5 → 6. The highlighted bond lengths are in units of Ångström. See text for details.

same number of halogen/CF₃ substituents. This can be rationalized by the fact that the total number of fluorine atoms, and associated electron-withdrawing effect, in *Z*- and *E*-CF₃CH=CHCF₃ is double that found in *Z*- and *E*-CF₃CH=CHCl. Furthermore, greater steric hindrance is associated with the CF₃ group than that from the Cl atom. In the case of CF₃CF=CHF, the *E*-isomer has a greater reactivity than the *Z*-isomer towards Cl atoms, OH radicals and O₃, so no general *Z*- versus *E*-isomer trend can be assessed from the data in Table 2. Further experimental and computational studies of general trends in HFO reactivity would be of interest, but beyond the scope of the present study.

3.6 Computational study of the reactivity of OH and OD radicals

The calculated geometries of the reactant alkenes, *Z*- and *E*-CF₃CH=CHCF₃, are shown in Fig. 5 together with the geometries of the reaction complexes between the OH radical and the alkenes, the product alkyl radicals, and the connecting transition states. It is worth noting that the transition state in each case closely resembles the OH-alkene complex. We also note that the *Z*-isomer gives rise to the transition state resembling the complex closest, which is most likely due to the larger strain release in this case, which gives an energetic bonus earlier during the progress of the addition. The free energy changes relative to

Table 3 Free energy changes associated with the formation of CF₃CH=CHCF₃-OH/OD complexes and the formation of alkyl radicals from the complexes as well as the free energy changes associated with the formation of alkyl radicals from the reactions with Cl atoms^a

	$\Delta_r G$ (complex)	$\Delta_r G^\ddagger$ (barrier)	$\Delta_r G$ (alkyl radical)
<i>E</i> -CF ₃ CH=CHCF ₃ + OH	5.2	22.6	-98.1
<i>E</i> -CF ₃ CH=CHCF ₃ + OD	4.9	22.1	-99.6
<i>Z</i> -CF ₃ CH=CHCF ₃ + OH	2.7	7.5	-112.5
<i>Z</i> -CF ₃ CH=CHCF ₃ + OD	2.5	7.3	-114.1
<i>E</i> -CF ₃ CH=CHCF ₃ + Cl	—	—	-57
<i>Z</i> -CF ₃ CH=CHCF ₃ + Cl	—	—	-60

^a G4MP2 values in kJ mol⁻¹ at 298.15 K.

the separated reactants (alkene + OH and alkene + OD) are shown in Table 3. The formation of a complex between the *E*-isomer and the OH radical is endothermic by approximately 5.2 kJ mol⁻¹ and there is a barrier for formation of the alkyl radical of 22.6 kJ mol⁻¹. The overall reaction is exothermic by -98.1 kJ mol⁻¹.

The OD equivalent gives rise to a slightly more weakly bound complex (by 0.3 kJ mol⁻¹) and a barrier, which is slightly lower (0.5 kJ mol⁻¹). The formation of the alkyl radical on the other hand is more exothermic by 1.5 kJ mol⁻¹. In the case of the *Z*-isomer the barriers and the endothermicities of formation are



significantly reduced. The barrier for the formation of the alkyl radical from the $\text{RCF}_3\text{-HO}$ adduct is 7.5 kJ mol^{-1} whereas the adduct is 2.7 kJ mol^{-1} less stable than the separated reactants. The alkyl radical is more stable than the reactants by $-112.5 \text{ kJ mol}^{-1}$ and the increased stability reflects release of strain from the *Z*-isomer. The effect of the deuterium substitution is slightly reduced compared to the *E*-isomer. The barrier for the OD addition is lower by 0.2 kJ mol^{-1} . The values are summarized in Table 3. The lower barrier in the case of OD is attributed to the generally weaker hydrogen bonds that are in play when a hydrogen is replaced by a deuterium.

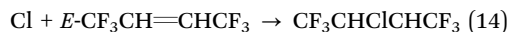
The relative barrier difference for OH *versus* OD addition is in qualitative agreement with experimental finding that OD addition proceeds faster than OH addition in the sense that the barrier for OD addition is smaller for both *Z*- and *E*- $\text{CF}_3\text{CH=CHCF}_3$. The experimental result that the effect is smaller in the case of the *Z*-isomer is also in agreement with the calculations, because the calculated barrier is less impacted by isotope substitution in the *Z*-isomer case. At a first glance, the barrier differences seem small compared to the experimental relative rate coefficients. To assess the impact on the rate coefficients we evaluated the ratios of $k_{\text{OD}}/k_{\text{OH}}$ for both *Z*- and *E*- $\text{CF}_3\text{CH=CHCF}_3$ from the partition functions, Q , and barrier differences using the equation:

$$\frac{k_{\text{OD}}}{k_{\text{OH}}} = \frac{Q_{\text{OH}}(\text{TS}) \times Q_{\text{OD}}(\text{complex})}{Q_{\text{OH}}(\text{complex}) \times Q_{\text{OD}}(\text{TS})} \times e^{\Delta\Delta G^\ddagger} \quad (\text{III})$$

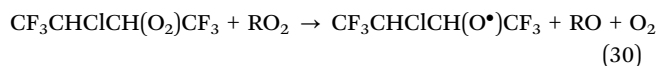
where TS is the transition state, complex is the OH/OD-alkene complexes, subscripts on the partition functions denote either the OH or OD radical reaction, and $\Delta\Delta G^\ddagger$ is the difference between the barrier heights to form the alkyl radical products. The $k_{\text{OD}}/k_{\text{OH}}$ ratio is found to be 1.8 for *E*- $\text{CF}_3\text{CH=CHCF}_3$ and 1.1 for *Z*- $\text{CF}_3\text{CH=CHCF}_3$. This trend is consistent with the experimental results, showing a larger difference between the OD and OH rate coefficients for *E*- $\text{CF}_3\text{CH=CHCF}_3$ than for *Z*- $\text{CF}_3\text{CH=CHCF}_3$. The calculated total energies and optimized geometries can be found in the ESI† (Tables S1 and S2).

3.7 Product study of *E*- $\text{CF}_3\text{CH=CHCF}_3 + \text{Cl}$

The initial reaction mixtures for the product study of the reaction $\text{E-CF}_3\text{CH=CHCF}_3 + \text{Cl}$ consisted of 2.61–4.07 mTorr *E*- $\text{CF}_3\text{CH=CHCF}_3$ and 73.2–89.0 mTorr Cl_2 in 700 Torr air/ N_2/O_2 diluent. The mixtures were subjected to a total of 33–52 seconds of UV irradiation. The reaction proceeds with the addition of a Cl atom to the double bond creating an alkyl radical, that will react with O_2 forming a peroxy radical (RO_2):



The peroxy radical can react with other peroxy radicals, itself or NO (if present), to form an alkoxy radical (RO):



The alkoxy radical can then react with O_2 to give a ketone or decompose *via* C–C bond scission to give a CF_3CHCl radical and CF_3CHO . CF_3CHCl will react with O_2 giving $\text{CF}_3\text{C}(\text{O})\text{Cl}$:

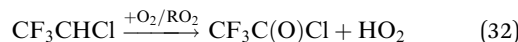


Fig. 6 shows spectra of a mixture of 2.61 mTorr *E*- $\text{CF}_3\text{CH=CHCF}_3$ and 73.2 mTorr Cl_2 in 700 Torr air, before (panel A) and after (panel B) 24 seconds of UV irradiation. 59% of *E*- $\text{CF}_3\text{CH=CHCF}_3$ was consumed in the irradiation. Panel E is a residual spectrum obtained by subtracting all remaining *E*- $\text{CF}_3\text{CH=CHCF}_3$ from panel B (panel B – $0.41 \times$ panel A). IR features present in panel E are assigned to $\text{CF}_3\text{CHClC}(\text{O})\text{CF}_3$, as the only observed product. While we do not have sample of $\text{CF}_3\text{CHClC}(\text{O})\text{CF}_3$ with which to

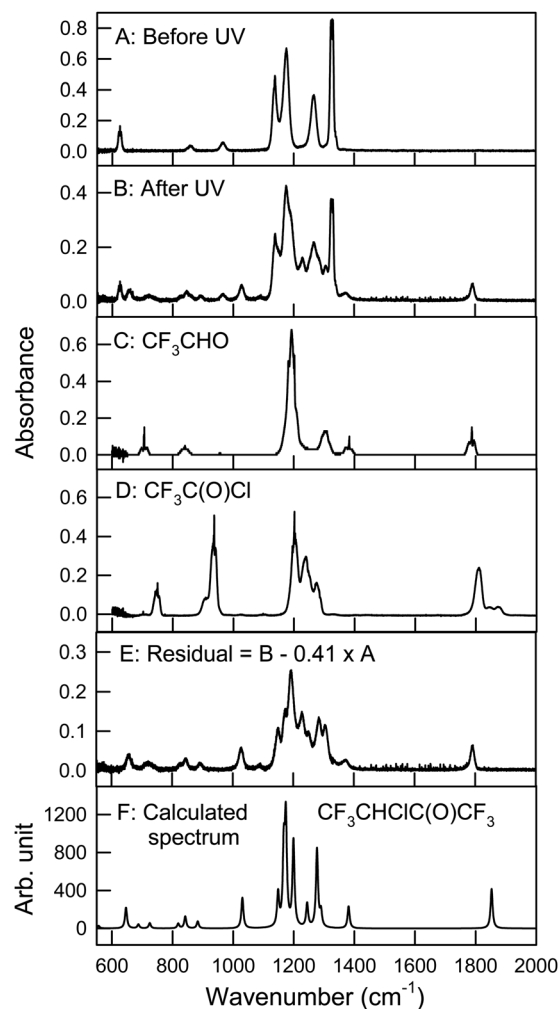


Fig. 6 Panel A: IR spectrum of 2.61 mTorr *E*- $\text{CF}_3\text{CH=CHCF}_3$ and 73.2 mTorr Cl_2 before UV irradiation, panel B: spectrum of the reaction mixture after 24 seconds UV irradiation, panel C: reference spectrum of CF_3CHO , panel D: reference spectrum of $\text{CF}_3\text{C}(\text{O})\text{Cl}$, panel E: residual spectrum (panel B – $0.41 \times$ panel A) assigned to $\text{CF}_3\text{CHClC}(\text{O})\text{CF}_3$, and panel F: calculated IR spectrum of $\text{CF}_3\text{CHClC}(\text{O})\text{CF}_3$ at the B3LYP/6-31+G(d,p) level. See text for details.



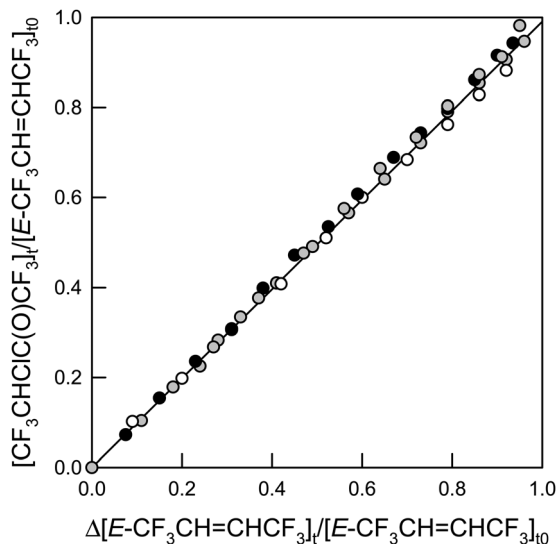


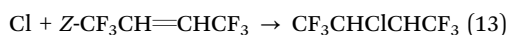
Fig. 7 Formation of $\text{CF}_3\text{CHClC}(\text{O})\text{CF}_3$ versus the loss of $E\text{-CF}_3\text{CH}=\text{CHCF}_3$ in the presence of Cl atoms. The shades indicate the O_2 partial pressure: 16 Torr (white), 140 Torr (gray), and 700 Torr (black) in a total of 700 Torr made up with air or N_2 .

obtain a genuine reference spectrum, a calculated spectrum of the compound is shown in panel F. This and other spectra were calculated using the GAUSSIAN 09 suite of programs, revision D.01 at the B3LYP/6-31+G(d,p) level (see below).¹² No formation of CF_3CHO (panel C) or $\text{CF}_3\text{C}(\text{O})\text{Cl}$ (panel D) was observed in these experiments. Upper limits for the yields of CF_3CHO and $\text{CF}_3\text{C}(\text{O})\text{Cl}$ were determined as 1% for both compounds. Therefore, we conclude that reaction (31b) is not significant in the Cl atom initiated degradation. Fig. 7 shows the formation of $\text{CF}_3\text{CHClC}(\text{O})\text{CF}_3$ as a function of the loss of $E\text{-CF}_3\text{CH}=\text{CHCF}_3$ in the presence of Cl atoms.

Calculated spectra of $E\text{-CF}_3\text{CH}=\text{CHCF}_3$ and several conformers of $\text{CF}_3\text{CHClC}(\text{O})\text{CF}_3$ were calculated at the B3LYP/6-31+G(d,p) level. One conformer of $\text{CF}_3\text{CHClC}(\text{O})\text{CF}_3$ was calculated at the $\omega\text{B97XD/cc-pVTZ}$ level being in agreement with the other calculations. The optimized geometries and IR spectra are shown in the ESI† (Tables S3–S8 and Fig. S2–S7).

3.8 Product study of $Z\text{-CF}_3\text{CH}=\text{CHCF}_3 + \text{Cl}$

A product study of the reaction of $Z\text{-CF}_3\text{CH}=\text{CHCF}_3 + \text{Cl}$ was performed using initial reaction mixtures of 1.12–1.91 mTorr $Z\text{-CF}_3\text{CH}=\text{CHCF}_3$, 75.4–87.3 mTorr Cl_2 , and 0 or 10.4 mTorr NO in 700 Torr air or O_2 diluent. The mixtures were subjected to a total of 17–29 seconds of UV irradiation. The reaction of $Z\text{-CF}_3\text{CH}=\text{CHCF}_3 + \text{Cl}$ is initiated by the addition of Cl atoms to the double bond of $Z\text{-CF}_3\text{CH}=\text{CHCF}_3$ creating an alkyl radical as for $E\text{-CF}_3\text{CH}=\text{CHCF}_3$ in reaction (14).



After addition of the Cl atom, the Z/E isometry is lost, free rotation of the C–C bond is possible, and the following reactions in the degradation of the Z -isomer will be the same as observed for the E -isomer in reactions (29)–(32).

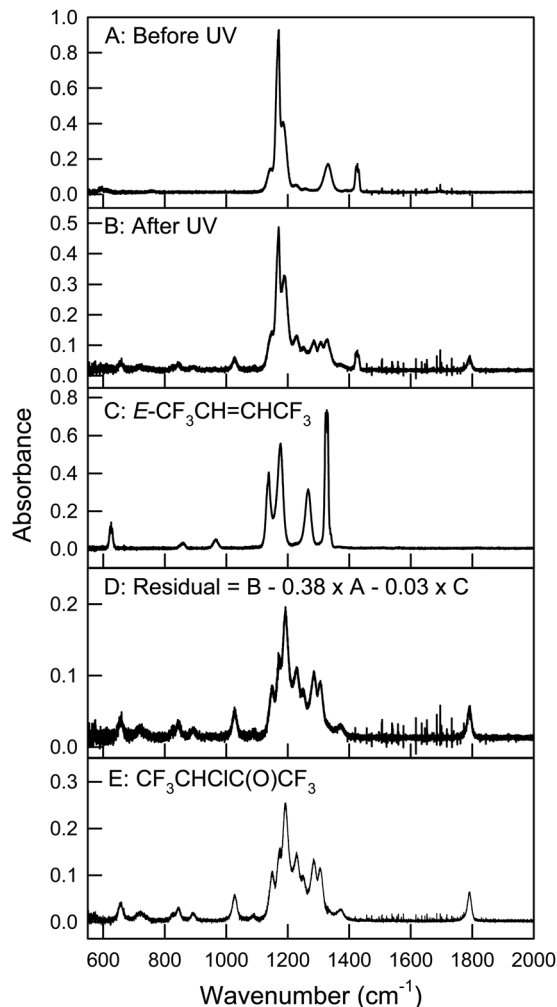


Fig. 8 Panel A: A mixture of 1.91 mTorr $Z\text{-CF}_3\text{CH}=\text{CHCF}_3$ and 75.4 mTorr Cl_2 in 700 Torr air before UV irradiation, panel B: the reaction mixture after 17 seconds UV irradiation, panel C: reference spectrum of $E\text{-CF}_3\text{CH}=\text{CHCF}_3$, panel D: residual spectrum obtained from subtracting features of Z - and $E\text{-CF}_3\text{CH}=\text{CHCF}_3$ (panel B – 0.38 × panel A – 0.03 × panel C) assigned to $\text{CF}_3\text{CHClC}(\text{O})\text{CF}_3$, and panel E: spectrum of $\text{CF}_3\text{CHClC}(\text{O})\text{CF}_3$ obtained from the product study of $E\text{-CF}_3\text{CH}=\text{CHCF}_3$ in the presence of Cl atoms. See text for details.

Fig. 8 shows spectra of a reaction mixture of 1.91 mTorr $Z\text{-CF}_3\text{CH}=\text{CHCF}_3$ and 75.4 mTorr Cl_2 in 700 Torr air, before (panel A) and after (panel B) 17 seconds of UV irradiation. 62% of $Z\text{-CF}_3\text{CH}=\text{CHCF}_3$ was consumed in the irradiation. Panel C shows a reference spectrum of $E\text{-CF}_3\text{CH}=\text{CHCF}_3$ and panel D is a residual spectrum obtained by subtracting all remaining features of $Z\text{-CF}_3\text{CH}=\text{CHCF}_3$ (0.38 × panel A) and $E\text{-CF}_3\text{CH}=\text{CHCF}_3$ (0.03 × panel C) from panel B. This spectrum is assigned to $\text{CF}_3\text{CHClC}(\text{O})\text{CF}_3$. Panel E shows the residual spectrum of $\text{CF}_3\text{CHClC}(\text{O})\text{CF}_3$ obtained from the product study of $E\text{-CF}_3\text{CH}=\text{CHCF}_3$.

Fig. 9 shows the formation of $\text{CF}_3\text{CHClC}(\text{O})\text{CF}_3$ and $E\text{-CF}_3\text{CH}=\text{CHCF}_3$ versus the loss of $Z\text{-CF}_3\text{CH}=\text{CHCF}_3$. The shades of the symbols indicate different O_2 partial pressures and the presence or absence of NO. No effect of varying the O_2



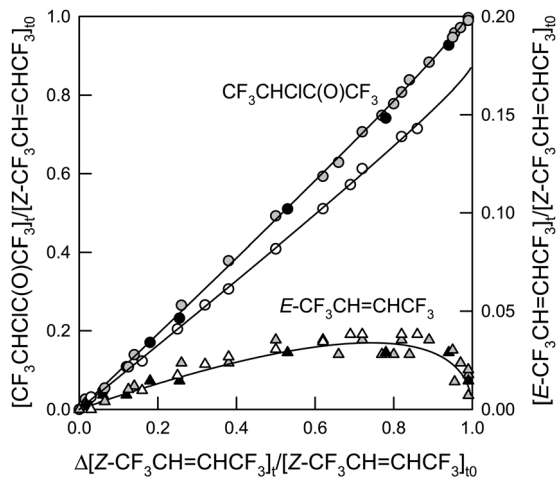
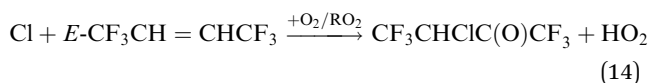
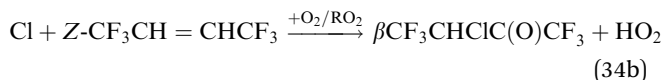
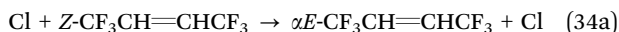


Fig. 9 Formation of $\text{CF}_3\text{CHClC(O)CF}_3$ (circles, left y-axis) and $E\text{-CF}_3\text{CH}=\text{CHCF}_3$ (triangles, right y-axis) versus the loss of $Z\text{-CF}_3\text{CH}=\text{CHCF}_3$ in the presence of Cl atoms in a total of 700 Torr air in the absence (gray) and presence (white) of NO or 700 Torr O_2 in the absence of NO (black). The lines are non-linear fits to the data. See text for details.

partial pressure was observed. The formation of $E\text{-CF}_3\text{CH}=\text{CHCF}_3$ is evidence of isomerization. After a Cl atom has added to the double bond in $Z\text{-CF}_3\text{CH}=\text{CHCF}_3$ (reaction (13)), the center C–C bond has free rotation and the double bond will reform to the more stable E -conformation in competition with reaction (29) expelling a Cl atom:



As discussed in Section 3.7 $E\text{-CF}_3\text{CH}=\text{CHCF}_3$ reacts with Cl to give 100% $\text{CF}_3\text{CHClC(O)CF}_3$. No evidence of isomerization was observed in the degradation of $E\text{-CF}_3\text{CH}=\text{CHCF}_3$. During the course of the reaction of $Z\text{-CF}_3\text{CH}=\text{CHCF}_3$ with Cl atoms the apparent yield of $E\text{-CF}_3\text{CH}=\text{CHCF}_3$ decreases and the concentration of $\text{CF}_3\text{CHClC(O)CF}_3$ increases in a non-linear way. Fits to the data are based on reactions (34a), (34b) and (14):



Here α and β are the initial yields of $E\text{-CF}_3\text{CH}=\text{CHCF}_3$ and $\text{CF}_3\text{CHClC(O)CF}_3$, respectively. A method described by Meagher *et al.*,²⁰ is used to fit the $E\text{-CF}_3\text{CH}=\text{CHCF}_3$ and $\text{CF}_3\text{CHClC(O)CF}_3$ data. The equation describing the fractional conversion of Z - to $E\text{-CF}_3\text{CH}=\text{CHCF}_3$ is:

$$\frac{[E\text{-CF}_3\text{CH}=\text{CHCF}_3]_t}{[Z\text{-CF}_3\text{CH}=\text{CHCF}_3]_0} = \frac{\alpha}{1 - \frac{k_{14}}{k_{34}}} (1-x) \left\{ (1-x)^{(k_{14}/k_{34}-1)} - 1 \right\} \quad (IV)$$

Here k_{34} and k_{14} are the rate coefficients of the reactions of Cl + Z - and $E\text{-CF}_3\text{CH}=\text{CHCF}_3$ determined above, where

$k_{34} = k_{13}$, and x is the conversion of $Z\text{-CF}_3\text{CH}=\text{CHCF}_3$, defined as:

$$x \equiv 1 - \frac{[Z\text{-CF}_3\text{CH}=\text{CHCF}_3]_t}{[Z\text{-CF}_3\text{CH}=\text{CHCF}_3]_0} = \frac{\Delta[Z\text{-CF}_3\text{CH}=\text{CHCF}_3]_t}{[Z\text{-CF}_3\text{CH}=\text{CHCF}_3]_0} \quad (V)$$

In this fit, the k_{14}/k_{13} ratio is known, so this value is fixed to be:

$$\frac{k_{14}}{k_{13}} = \frac{1.36 \times 10^{-11} \text{ cm}^3 \text{ molecule}^{-1} \text{ s}^{-1}}{2.59 \times 10^{-11} \text{ cm}^3 \text{ molecule}^{-1} \text{ s}^{-1}} = 0.526 \quad (VI)$$

This gives an initial yield of $E\text{-CF}_3\text{CH}=\text{CHCF}_3$ of $\alpha = (6.9 \pm 0.8)\%$. The fit to the $\text{CF}_3\text{CHClC(O)CF}_3$ data uses eqn (IV) as a modification to a linear fit, accounting for reaction (14), describing the conversion of $Z\text{-CF}_3\text{CH}=\text{CHCF}_3$ to $\text{CF}_3\text{CHClC(O)CF}_3$:

$$\frac{[\text{CF}_3\text{CHClC(O)CF}_3]_t}{[Z\text{-CF}_3\text{CH}=\text{CHCF}_3]_0} = \beta x + \alpha x - \frac{\alpha}{1 - \frac{k_{14}}{k_{34}}} (1-x) \left\{ (1-x)^{(k_{14}/k_{34}-1)} - 1 \right\} \quad (VII)$$

Fitting eqn (VII) to the $\text{CF}_3\text{CHClC(O)CF}_3$ data with the known values of k_{14}/k_{13} and α , the initial yield of $\text{CF}_3\text{CHClC(O)CF}_3$ is $\beta = (95 \pm 10)\%$ in the absence of NO. Combining the initial yields of $E\text{-CF}_3\text{CH}=\text{CHCF}_3$ and $\text{CF}_3\text{CHClC(O)CF}_3$ mass balance is obtained. It is clear that at atmospheric pressure, the dominant pathway of the reaction of Cl + $Z\text{-CF}_3\text{CH}=\text{CHCF}_3$ is *via* reaction (34b).

In the presence of NO the yield of $\text{CF}_3\text{CHClC(O)CF}_3$ is slightly decreased compared to the experiments in the absence of NO. The yield of $E\text{-CF}_3\text{CH}=\text{CHCF}_3$ is not affected by the presence of NO, so eqn (VII) can be used to fit the $\text{CF}_3\text{CHClC(O)CF}_3$ data using the known values of k_{14}/k_{13} and α . This gives an initial yield of $\text{CF}_3\text{CHClC(O)CF}_3$ of $\beta = (81 \pm 8)\%$ in the presence of NO. The formation of ClNO and ClNO₂ was observed in these experiments. A minor product with an IR absorption peak at 1699 cm^{-1} was observed, which, assuming conserved mass balance, could have a yield of 12%. This compound was not positively identified, but could be due to the formation of an organic nitrate compound.

While we did not perform any comprehensive OH radical initiated product studies of Z - and $E\text{-CF}_3\text{CH}=\text{CHCF}_3$, Baasandorj *et al.* identified some products of the reaction of $Z\text{-CF}_3\text{CH}=\text{CHCF}_3$ with OH radicals.⁷ They observed C(O)F₂ and CF_3CHO as the main F-containing products, suggesting that C–C scission of the central carbon bond could be a more significant pathway in the atmospheric degradation initiated by OH radical than what we have been able to observe above in the Cl atom initiated reaction.

Calculated IR spectra of two conformers of $Z\text{-CF}_3\text{CH}=\text{CHCF}_3$ at the B3LYP/6-31+G(d,p) level are supplied in the ESI† (Tables S9, S10 and Fig. S8, S9) and show good agreement with the experimental spectrum.



3.9 Isomerization of *Z*- and *E*-CF₃CH=CHCF₃

Experiments were performed to investigate any potential isomerization in the reactions of *Z*-CF₃CH=CHCF₃ with OH or OD radicals giving *E*-CF₃CH=CHCF₃ as observed for the reaction of *Z*-CF₃CH=CHCF₃ with Cl atoms. Reaction mixtures consisting of 1.21–1.37 mTorr *Z*-CF₃CH=CHCF₃ and 43.9 mTorr CH₃ONO or 42.9 mTorr CD₃ONO in 700 Torr air diluent were subjected to a total of 110–210 seconds of UV irradiation. No formation of *E*-CF₃CH=CHCF₃ was observed in these experiments. Calculations were performed of the energy of the initial alkyl radical formed from the addition of Cl atoms to *Z*-CF₃CH=CHCF₃. The alkyl radical energy is approximately twice that of the alkyl radical formed with OH or OD radicals (see Table 3), making it more likely that the reaction can proceed in the reverse direction eliminating the Cl atom and reforming CF₃CH=CHCF₃. The *E*-isomer has less strain than the *Z*-isomer thus making it more likely to be formed. A similar calculation was performed of the alkyl radical formed from the reaction of Cl + *E*-CF₃CH=CHCF₃. The energy of this initial alkyl radical is slightly smaller than that from the *Z*-isomer (see Table 3), but in the experiments, no isomerization was observed. The optimized structures of both initial alkyl radicals formed from Cl atoms are shown in Fig. S11 in the ESI.† Comparing the barriers of formation of the alkyl radicals from the OH/OD radical additions, the *E*-isomer barriers are more than double those of the *Z*-isomer, making the barriers the potential limiting factor of isomerization. Similar barriers can be expected from the Cl atom additions to *Z*- and *E*-CF₃CH=CHCF₃, explaining why no isomerization was observed for the reaction Cl + *E*-CF₃CH=CHCF₃. It would be expected that *E*-CF₃CH=CHCF₃ will not isomerize in the reactions with OH or OD radicals for the same reasons as discussed above. No additional experiments were performed with OH/OD + *E*-CF₃CH=CHCF₃ besides the ones used for determining the rate coefficients.

3.10 Product study of CF₃CHClC(O)CF₃ + Cl

To further investigate the oxidation of the primary product, CF₃CHClC(O)CF₃, experiments were conducted in which all of the starting material, *Z*-CF₃CH=CHCF₃, was allowed to react with Cl to generate CF₃CHClC(O)CF₃. Only then, the loss of CF₃CHClC(O)CF₃ and the subsequent formation of products was monitored, normalizing the products to the initial concentration of CF₃CHClC(O)CF₃. All *E*-CF₃CH=CHCF₃ had also reacted at this point. The initial reaction mixtures were 1.12–1.91 mTorr *Z*-CF₃CH=CHCF₃ and 75.4–87.3 mTorr Cl₂ in 700 Torr air or O₂. The mixtures were subjected to a total of 3150–5400 seconds of UV irradiation after all *Z*-CF₃CH=CHCF₃ was converted to CF₃CHClC(O)CF₃. Three products are observed in the degradation of CF₃CHClC(O)CF₃: CF₃C(O)Cl, C(O)F₂, and CF₃O₃CF₃. Fig. 10 shows IR spectra recorded before (panel A) and after (panel B) UV irradiation of a mixture of CF₃CHClC(O)CF₃ and Cl₂. Panel C shows the resulting spectrum after subtracting all features of CF₃CHClC(O)CF₃ in panel A from panel B (panel B – 0.56 × panel A). Panels D and E show reference spectra of C(O)F₂ and CF₃C(O)Cl, respectively. The residual

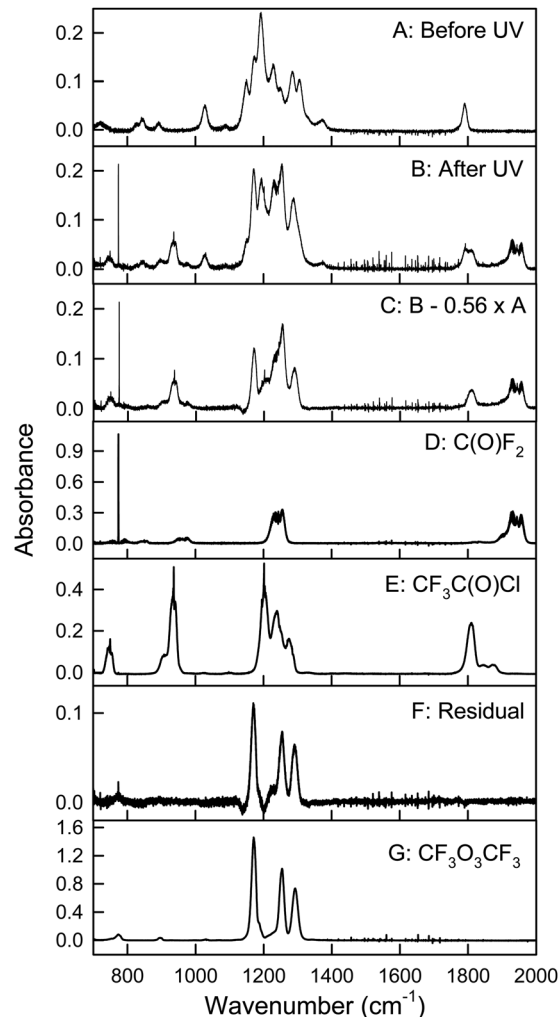


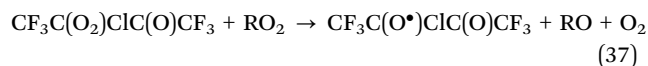
Fig. 10 Panel A: IR spectrum of CF₃CHClC(O)CF₃ + Cl₂ before UV irradiation, panel B: spectrum of the reaction mixture after 25 minutes of UV irradiation, panel C: the resulting spectrum of subtracting the remaining features of CF₃CHClC(O)CF₃ from panel B (panel B – 0.56 × panel A), panel D: reference spectrum of C(O)F₂, panel E: reference spectrum of CF₃C(O)Cl, panel F: residual spectrum, when subtracting C(O)F₂ and CF₃C(O)Cl from panel C, and panel G: reference spectrum of CF₃O₃CF₃. The residual spectrum in panel F is assigned to CF₃O₃CF₃. See text for details.

obtained when subtracting features of C(O)F₂ and CF₃C(O)Cl from panel C is shown in panel F. Panel G shows a reference spectrum of CF₃O₃CF₃. The residual spectrum is assigned to CF₃O₃CF₃, and quantified as such.²¹

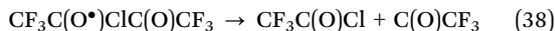
The degradation of CF₃CHClC(O)CF₃ is initiated by Cl atoms by abstraction of the hydrogen atom forming an alkyl radical that reacts with O₂ forming a peroxy radical:



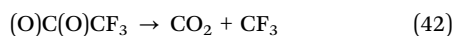
The peroxy radical will then react with itself or NO (if present) or another peroxy radical forming an alkoxy radical:



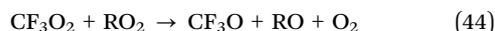
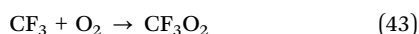
The alkoxy radical formed will break by C–C scission to give $\text{CF}_3\text{C}(\text{O})\text{Cl}$ and a $\text{C}(\text{O})\text{CF}_3$ radical that will either decompose to give CO and a CF_3 radical or react with O_2 to give a peroxy radical:



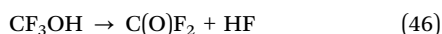
The alkyl radical, $\text{C}(\text{O})\text{CF}_3$, will predominantly react with O_2 (97% under laboratory conditions, 99.5% in the atmosphere) *via* reaction (40) and the remainder (3% or 0.5%) will decompose *via* reaction (39).²² The peroxy radical formed in reaction (40) will then react with itself or another peroxy radical giving an alkoxy radical, which decomposes to give a CF_3 radical and CO_2 :²²



The CF_3 radical will react with O_2 forming a peroxy radical that can react with another peroxy radical to give an alkoxy radical and O_2 :



The formed alkoxy radical CF_3O can abstract a hydrogen atom from a hydrocarbon (RH) forming an alcohol. This alcohol will eliminate HF forming $\text{C}(\text{O})\text{F}_2$:



The peroxy radical CF_3O_2 and the alkoxy radical CF_3O can also react with each other forming the trioxide $\text{CF}_3\text{O}_3\text{CF}_3$ (bis(trifluoromethyl)trioxide):



Fig. 11 shows the formation of products *versus* the loss of $\text{CF}_3\text{CHClC}(\text{O})\text{CF}_3$. The solid lines through the $\text{CF}_3\text{C}(\text{O})\text{Cl}$ data are linear least squares analyses of the data. The slopes give yields of $\text{CF}_3\text{C}(\text{O})\text{Cl}$ of $(78 \pm 8)\%$ in the experiments where UVB lamps were used for Cl_2 photolysis and $(102 \pm 10)\%$ when using UVA lamps to photolyze Cl_2 . The dotted lines through the $\text{C}(\text{O})\text{F}_2$ and $\text{CF}_3\text{O}_3\text{CF}_3$ data are trend lines to serve as visual aids for inspection of the data. As a measure of the combined yield of CF_3 radicals formed in the degradation of $\text{CF}_3\text{CHClC}(\text{O})\text{CF}_3$, diamonds show the sum of the fractional formation of $\text{C}(\text{O})\text{F}_2$ and twice the fractional formation of $\text{CF}_3\text{O}_3\text{CF}_3$. As described above the CF_3 radicals will eventually give either $\text{C}(\text{O})\text{F}_2$ or $\text{CF}_3\text{O}_3\text{CF}_3$. $\text{CF}_3\text{O}_3\text{CF}_3$ will react on the walls of the chamber and form two $\text{C}(\text{O})\text{F}_2$ molecules. This is evidenced in Fig. 11, by the decrease in the slopes of formation of $\text{CF}_3\text{O}_3\text{CF}_3$ and the increase in the slopes of the formation of $\text{C}(\text{O})\text{F}_2$ during the course of the experiments. The solid lines through the diamonds in Fig. 11 are linear regressions giving yields of CF_3 radicals of $(95 \pm 10)\%$ and $(122 \pm 13)\%$ for the experiments using UVA and UVB lamps,

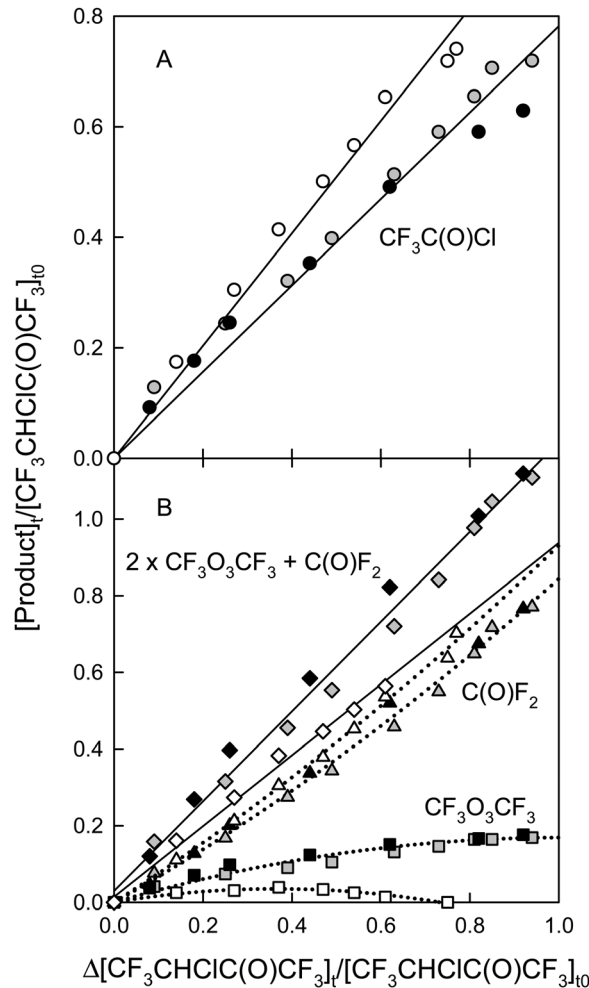
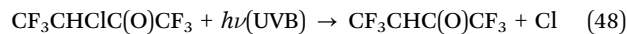


Fig. 11 Panel A: Formation of $\text{CF}_3\text{C}(\text{O})\text{Cl}$ (circles) *versus* the loss of $\text{CF}_3\text{CHClC}(\text{O})\text{CF}_3$ in the presence of Cl atoms in a total of 700 Torr air using UVA (white) or UVB (gray) lamps and 700 Torr O_2 using UVB lamps (black). Panel B: $\text{C}(\text{O})\text{F}_2$ (triangles), and $\text{CF}_3\text{O}_3\text{CF}_3$ (squares) *versus* the loss of $\text{CF}_3\text{CHClC}(\text{O})\text{CF}_3$ in the presence of Cl atoms in a total of 700 Torr air using UVA (white) or UVB (gray) lamps and 700 Torr O_2 using UVB lamps (black). The diamond symbols are the sum of CF_3 radicals formed ($2 \times \text{CF}_3\text{O}_3\text{CF}_3 + \text{C}(\text{O})\text{F}_2$). The solid lines are linear fits to the data and the dotted lines are trend lines through the data to ease visual inspection of the data, see text for details.

respectively. UVB lights are expected to photolyze $\text{CF}_3\text{CHClC}(\text{O})\text{CF}_3$, as has been observed for similar fluorinated ketones.^{23,24} The products observed in the experiments using UVB lamps are therefore a combination of the reaction with Cl atoms and of the photolysis. The experiment using UVA lamps gives products of the reaction with Cl atoms only. Here, the yield of the reaction is indistinguishable from 100% of $\text{CF}_3\text{C}(\text{O})\text{Cl}$ and the co-formed CF_3 radical (observed as $\text{C}(\text{O})\text{F}_2$ and $\text{CF}_3\text{O}_3\text{CF}_3$). In the experiments using UVB lamps, $(78 \pm 8)\%$ of the loss of $\text{CF}_3\text{CHClC}(\text{O})\text{CF}_3$ is *via* reaction with Cl atoms observed as $\text{CF}_3\text{C}(\text{O})\text{Cl}$ and the remaining is loss by photolysis. The photolysis of $\text{CF}_3\text{CHClC}(\text{O})\text{CF}_3$ gives an alkoxy radical that will break into two radicals, CF_3CH and $\text{C}(\text{O})\text{CF}_3$:



The CF_3CH radical will react with O_2 forming a peroxy radical and then proceed to react with another peroxy radical to form CF_3CHO :



CF_3CHO has a fast reaction with Cl giving a $\text{C}(\text{O})\text{CF}_3$ radical:^{25,26}



The $\text{C}(\text{O})\text{CF}_3$ radical decomposition will follow the reaction pathway outlined in reactions (39)–(47) yielding a CF_3 radical that will react to give either $\text{C}(\text{O})\text{F}_2$ or $\text{CF}_3\text{O}_3\text{CF}_3$. The total observed formation of CF_3 radicals in the experiments with UVB lamps is 122% (as mentioned above). Of this, 78% is the co-product of $\text{CF}_3\text{C}(\text{O})\text{Cl}$ from the Cl atom reaction, leaving 44% CF_3 radicals formed from the photolysis of $\text{CF}_3\text{CHClC}(\text{O})\text{CF}_3$. The photolysis of $\text{CF}_3\text{CHClC}(\text{O})\text{CF}_3$ and the reaction with Cl atoms balances the mass in the experiments using UVB lamps. No change in the product yields was observed with an O_2 partial pressure varying between 140 and 700 Torr.

3.11 Atmospheric lifetimes of *Z*- and *E*- $\text{CF}_3\text{CH}=\text{CHCF}_3$

Compounds such as *Z*- and *E*- $\text{CF}_3\text{CH}=\text{CHCF}_3$ can leave the atmosphere *via* photolysis, wet and dry deposition or reaction with atmospheric oxidants: NO_3 radicals, O_3 , OH radicals and Cl atoms. *Z*- and *E*- $\text{CF}_3\text{CH}=\text{CHCF}_3$ does not absorb light in wavelengths < 200 nm, so photolysis in the troposphere is not important.²⁷ Compounds such as *Z*- and *E*- $\text{CF}_3\text{CH}=\text{CHCF}_3$ are likely to be in the gas phase rather than aqueous phase, so wet deposition is not likely to be an important atmospheric sink. The volatility of both compounds will render dry deposition unlikely as an atmospheric removal mechanism. The reaction with NO_3 radicals and O_3 is too slow to be of significance when compared to that of reaction with OH radicals and Cl atoms.²⁸ Even though the rate coefficients for the reactions of *Z*- and *E*- $\text{CF}_3\text{CH}=\text{CHCF}_3$ with Cl atoms are two orders of magnitude faster than those of the reactions with OH radicals, the reaction with OH radicals is the main sink for *Z*- and *E*- $\text{CF}_3\text{CH}=\text{CHCF}_3$. The global average atmospheric concentration of Cl atoms is generally low; approximately $[\text{Cl}] = 1 \times 10^3$ atom cm^{-3} ,²⁹ which is 3 orders of magnitude lower than the average global of OH radical concentration of $[\text{OH}] = 1 \times 10^6$ molecule cm^{-3} .³⁰ Locally Cl atom concentrations can be significantly higher, *e.g.* $[\text{Cl}] = 1.8 \times 10^4$ atom cm^{-3} in the marine boundary layer, so in some cases the Cl atom the reactions can compete with the OH radical reaction.³¹ The rate coefficients of the reactions with OH radicals determined here are at a temperature of 296 ± 2 K, but the appropriate temperature used to estimate atmospheric lifetimes based on OH radical reactions is 272 K.³² This needs to be considered when estimating the atmospheric lifetimes of the two compounds. Baasandorj *et al.* performed their study of the kinetics of the reaction of *Z*- $\text{CF}_3\text{CH}=\text{CHCF}_3 + \text{OH}$ radicals at temperatures of 212–374 K and found an Arrhenius expression for temperatures < 300 K giving $k_{19} = (5.19 \pm 0.53) \times 10^{-13}$ cm^3 molecule $^{-1}$ s $^{-1}$ at 272 K, showing a slight temperature

dependence.⁷ This value is indistinguishable from our value for k_{19} determined at here at $296 \text{ K} \pm 2 \text{ K}$. It is assumed that the reaction of *E*- $\text{CF}_3\text{CH}=\text{CHCF}_3 + \text{OH}$ will have a similar temperature dependency. Hence, we use the rate coefficients determined in this study at 296 ± 2 K to estimate atmospheric lifetimes of *Z*- and *E*- $\text{CF}_3\text{CH}=\text{CHCF}_3$ of 27 and 67 days, respectively. Baasandorj *et al.* estimated the lifetime of *Z*- $\text{CF}_3\text{CH}=\text{CHCF}_3$ as 22 days, in reasonable agreement with our present estimate.⁷

3.12 IR spectra, radiative efficiencies, and global warming potentials of *Z*- and *E*- $\text{CF}_3\text{CH}=\text{CHCF}_3$

The IR spectra in absorption cross section σ of *Z*- and *E*- $\text{CF}_3\text{CH}=\text{CHCF}_3$ are shown in Fig. 12. The integrated absorption cross sections of the two spectra ($550\text{--}2000$ cm^{-1}) have been determined to be $(2.51 \pm 0.13) \times 10^{-16}$ and $(2.96 \pm 0.15) \times 10^{-16}$ cm^2 molecule $^{-1}$, for *Z*- and *E*- $\text{CF}_3\text{CH}=\text{CHCF}_3$, respectively.

Using the method described by Pinnock *et al.*³³ the radiative efficiencies for *Z*- and *E*- $\text{CF}_3\text{CH}=\text{CHCF}_3$ were found to be 0.334 and 0.300 W m^{-2} ppb $^{-1}$, respectively. The value for *Z*- $\text{CF}_3\text{CH}=\text{CHCF}_3$ is in agreement with the value estimated by Baasandorj *et al.* of 0.38 W m^{-2} ppb $^{-1}$ using the same method.⁷ This method assumes that the gases are well-mixed in the atmosphere. For gases such as *Z*- and *E*- $\text{CF}_3\text{CH}=\text{CHCF}_3$ this is not the case since their atmospheric lifetime is not long enough for vertical mixing. Therefore we employ a correction factor, $f(\tau)$, dependent on the atmospheric lifetime of the compounds, τ , as described by Hodnebrog *et al.*,³⁴

$$f(\tau) = \frac{a\tau^b}{1 + c\tau^d} \quad (\text{VIII})$$

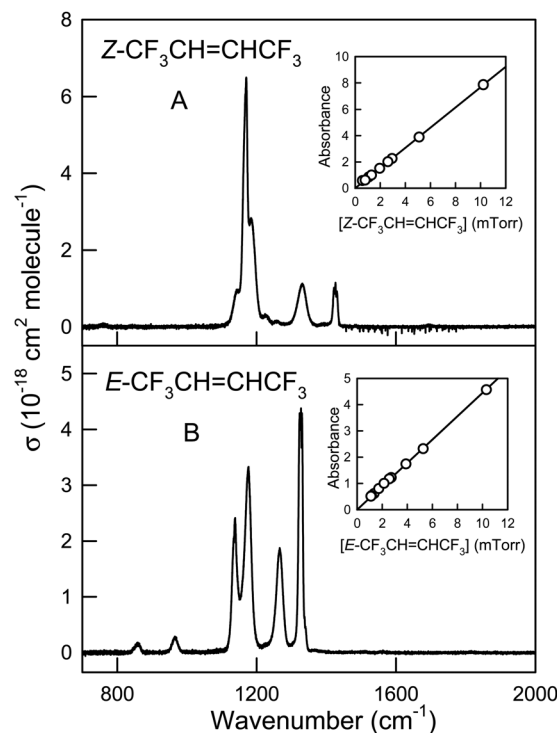


Fig. 12 IR spectra of 1.30 mTorr *Z*- $\text{CF}_3\text{CH}=\text{CHCF}_3$ (panel A) and 2.25 mTorr *E*- $\text{CF}_3\text{CH}=\text{CHCF}_3$ (panel B). The insets show the linearity of the absorbance.



where a , b , c , and d are constants with values of 2.962, 0.9312, 2.994, and 0.9302, respectively. The correction factors were calculated to be $f(\tau) = 0.21$ and 0.38 , for Z - and E - $\text{CF}_3\text{CH}=\text{CHCF}_3$ respectively. This gives effective values of the radiative efficiencies for Z - and

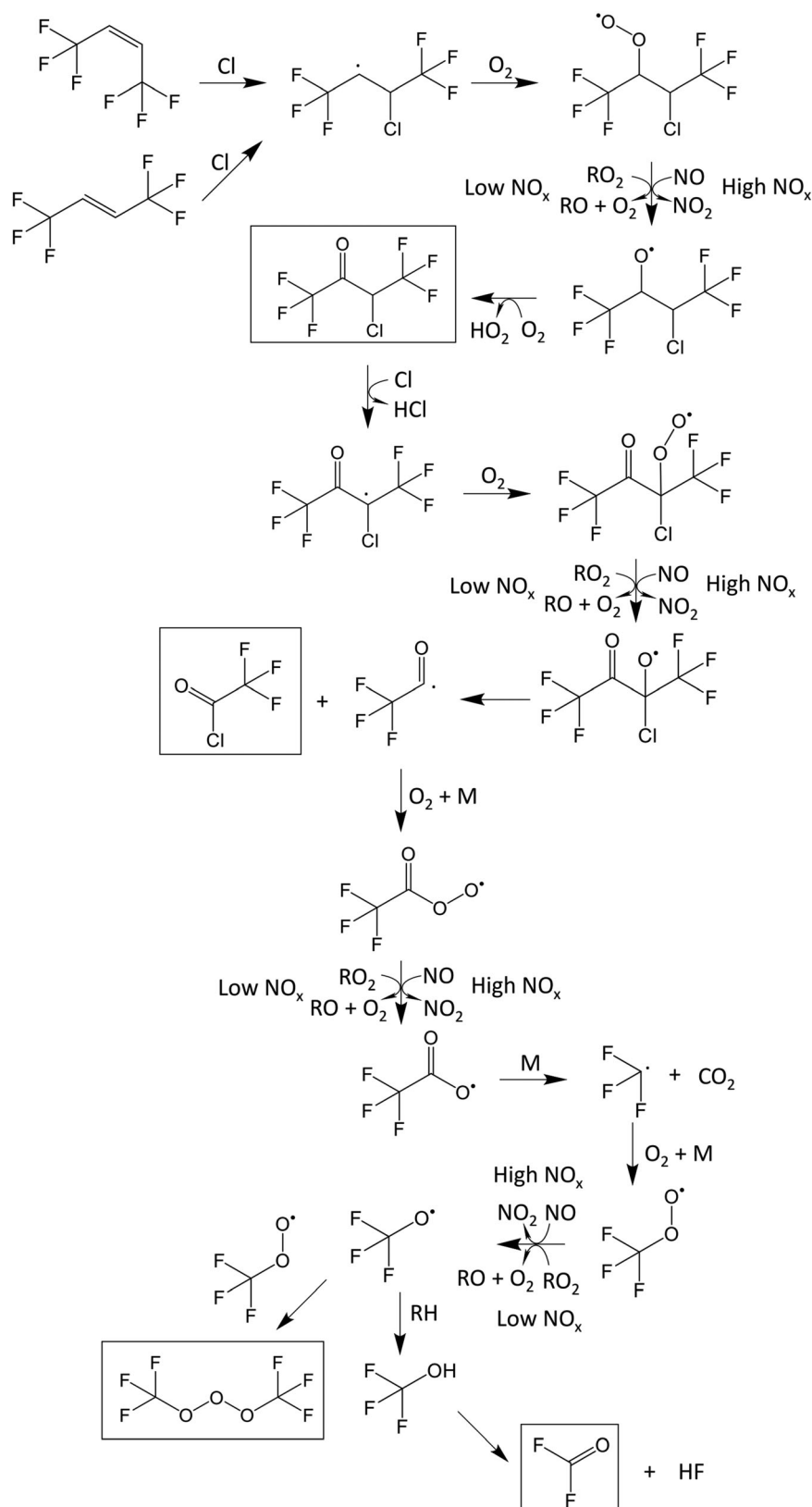


Fig. 13 Cl atom initiated degradation mechanism of Z - and E - $\text{CF}_3\text{CH}=\text{CHCF}_3$. The observed products are indicated by the boxes.



$E\text{-CF}_3\text{CH}=\text{CHCF}_3$ of 0.069 and 0.113 $\text{W m}^{-2} \text{ppb}^{-1}$, respectively. The radiative efficiencies and atmospheric lifetimes are used in the calculation of the global warming potentials (GWPs) of Z - and $E\text{-CF}_3\text{CH}=\text{CHCF}_3$ using the following equation,

$$\text{GWP}(x(t')) = \frac{\int_0^{t'} F_x \exp(-t/\tau_x) dt}{\int_0^{t'} F_{\text{CO}_2} R(t) dt} \quad (\text{IX})$$

where F_x is the radiative efficiency of x ($x = Z$ - or $E\text{-CF}_3\text{CH}=\text{CHCF}_3$), τ_x is the atmospheric lifetime of x with an exponential decay, t' is the time horizon (typically 20, 100, and 500 years), F_{CO_2} is the radiative efficiency of CO_2 , and $R(t)$ is a response function that describes the decay of an instantaneous pulse of CO_2 . The GWP is calculated relative to CO_2 mass for mass, and the denominator in eqn (IX) is the absolute global warming potential (AGWP) values of CO_2 . These have been determined to be $\text{AGWP}(\text{CO}_2) = 2.49 \times 10^{-14}$, 9.17×10^{-14} , and $32.2 \times 10^{-14} \text{ W year m}^{-2} \text{ kg}^{-1}$, ($= 0.196$, 0.722 , and $2.534 \text{ W year m}^{-2} \text{ ppb}^{-1}$) for 20, 100, and 500 year time horizons.³⁵ Thus we estimate the GWPs for $Z\text{-CF}_3\text{CH}=\text{CHCF}_3$ to be 6, 2, and 0 for time horizons of 20, 100, and 500 years, respectively. The GWPs for $E\text{-CF}_3\text{CH}=\text{CHCF}_3$ are estimated as 26, 7, and 2 for time horizons of 20, 100, and 500 years, respectively.

4. Conclusions and atmospheric impact

The present work provides a comprehensive description of the atmospheric chemistry and fate of Z - and $E\text{-CF}_3\text{CH}=\text{CHCF}_3$. The kinetics of the reactions of Z - and $E\text{-CF}_3\text{CH}=\text{CHCF}_3$ with Cl atoms, OH radicals, OD radicals, and O_3 have been determined. This is the first kinetic study of $E\text{-CF}_3\text{CH}=\text{CHCF}_3$ and the first determination of the rate coefficients of the reactions of $Z\text{-CF}_3\text{CH}=\text{CHCF}_3$ with Cl atoms and O_3 . Using the obtained rate coefficients for the reactions with OH radicals we find that both Z - and $E\text{-CF}_3\text{CH}=\text{CHCF}_3$ have short atmospheric lifetimes of 27 and 67 days, respectively. GWP values for both compounds are small; 2 and 7 for the 100 year time horizon for Z - and $E\text{-CF}_3\text{CH}=\text{CHCF}_3$, respectively. The Cl atom initiated degradation mechanism of Z - and $E\text{-CF}_3\text{CH}=\text{CHCF}_3$ is summarized in Fig. 13. For both Z - and $E\text{-CF}_3\text{CH}=\text{CHCF}_3$ the primary degradation product is $\text{CF}_3\text{CHClC}(\text{O})\text{CF}_3$. $E\text{-CF}_3\text{CH}=\text{CHCF}_3$ gives $\text{CF}_3\text{CHClC}(\text{O})\text{CF}_3$ in a yield indistinguishable from 100% and $Z\text{-CF}_3\text{CH}=\text{CHCF}_3$ gives $(95 \pm 10)\%$ $\text{CF}_3\text{CHClC}(\text{O})\text{CF}_3$ and $(7 \pm 1)\%$ $E\text{-CF}_3\text{CH}=\text{CHCF}_3$. $\text{CF}_3\text{CHClC}(\text{O})\text{CF}_3$ reacts with Cl atoms to give the secondary product $\text{CF}_3\text{C}(\text{O})\text{Cl}$ in a yield indistinguishable from 100%, co-formed with a CF_3 radical observed as $\text{C}(\text{O})\text{F}_2$ and $\text{CF}_3\text{O}_3\text{CF}_3$. Calculations were performed to investigate differences in the reactivities of Z - and $E\text{-CF}_3\text{CH}=\text{CHCF}_3$ towards OH and OD radicals and the observed isomerization of $Z\text{-CF}_3\text{CH}=\text{CHCF}_3$ giving $E\text{-CF}_3\text{CH}=\text{CHCF}_3$ in the experiments with Cl atoms. Energies of a pre-reaction complex, transition states and the formed alkyl radical were calculated for both alkenes for the reactions with OH and OD radicals as well as the energies of the alkyl radicals of the reaction of both alkenes with Cl atoms. The calculated energies are in good agreement with the experimental observations and in agreement

with the observed reactivity trends. Based on the short atmospheric lifetimes, the small GWP values and the non-toxic products of the Cl atom initiated degradation, the atmospheric impact of both Z - and $E\text{-CF}_3\text{CH}=\text{CHCF}_3$ is negligible. Further studies of the OH radical initiated products are needed to assess the atmospheric impact of the products formed by atmospheric degradation.

Acknowledgements

The authors thank Rajiv R. Singh (Honeywell) for supplying us with a sample of $Z\text{-CF}_3\text{CH}=\text{CHCF}_3$. We thank Mogens Brøndsted Nielsen and Martyn Jevric (University of Copenhagen) for supplying samples of CD_3ONO and $(\text{CH}_3)_2\text{CHONO}$ and for aid in the synthesis of CH_3ONO . Thanks are due to Timothy J. Wallington (Ford Motor Company) for kindly providing the absorption cross section of $\text{CF}_3\text{O}_3\text{CF}_3$.

References

- 1 M. J. Molina and F. S. Rowland, *Nature*, 1974, **249**, 810–812.
- 2 F. S. Rowland, *Ambio*, 1990, **19**, 281–292.
- 3 J. C. Farman, B. G. Gardiner and J. D. Shanklin, *Nature*, 1985, **315**, 207–210.
- 4 T. Midgley and A. L. Henne, *Ind. Eng. Chem.*, 1930, **22**, 542–545.
- 5 DuPont, *DuPont Develops HFO Foam Expansion Agent with Low Global Warming Potential, Additives for Polymers*, 2014, **6**, 2.
- 6 F. Molés, J. Navarro-Esbri, B. Peris, A. Mota-Babiloni, Á. Barragán-Cervera and K. Kontomaris, *Appl. Therm. Eng.*, 2014, **71**, 204–212.
- 7 M. Baasandorj, A. R. Ravishankara and J. B. Burkholder, *J. Phys. Chem. A*, 2011, **115**, 10539–10549.
- 8 E. J. K. Nilsson, C. Eskebjerg and M. S. Johnson, *Atmos. Environ.*, 2009, **43**, 3029–3033.
- 9 L. A. Curtiss, P. C. Redfern and K. Raghavachari, *J. Chem. Phys.*, 2007, **127**, 124105.
- 10 M. J. Frisch, G. W. Trucks, H. B. Schlegel, G. E. Scuseria, M. A. Robb, J. R. Cheeseman, G. Scalmani, V. Barone, B. Mennucci, G. A. Petersson, H. Nakatsuji, M. Caricato, X. Li, H. P. Hratchian, A. F. Izmaylov, J. Bloino, G. Zheng, J. L. Sonnenberg, M. Hada, M. Ehara, K. Toyota, R. Fukuda, J. Hasegawa, M. Ishida, T. Nakajima, Y. Honda, O. Kitao, H. Nakai, T. Vreven, J. J. A. Montgomery, J. E. Peralta, F. Ogliaro, M. Bearpark, E. B. J. J. Heyd, K. N. Kudin, V. N. Staroverov, R. Kobayashi, J. Normand, K. Raghavachari, A. Rendell, J. C. Burant, S. S. Iyengar, J. Tomasi, M. Cossi, N. Rega, J. M. Millam, M. Klene, J. E. Knox, J. B. Cross, V. Bakken, C. Adamo, J. Jaramillo, R. Gomperts, R. E. Stratmann, O. Yazyev, A. J. Austin, R. Cammi, C. Pomelli, J. W. Ochterski, R. L. Martin, K. Morokuma, V. G. Zakrzewski, G. A. Voth, P. Salvador, J. J. Dannenberg, S. Dapprich, A. D. Daniels, O. Farkas, J. B. Foresman, J. V. Ortiz, J. Cioslowski and D. J. Fox, *Gaussian 09, Revision A.02*, Gaussian Inc., Wallingford CT, 2009.
- 11 L. A. Curtiss, P. C. Redfern and K. Raghavachari, *Gaussian-4 Theory*, *J. Chem. Phys.*, 2007, **126**, 084108.



- 12 M. J. Frisch, G. W. Trucks, H. B. Schlegel, G. E. Scuseria, M. A. Robb, J. R. Cheeseman, G. Scalmani, V. Barone, B. Mennucci, G. A. Petersson, H. Nakatsuji, M. Caricato, X. Li, H. P. Hratchian, A. F. Izmaylov, J. Bloino, G. Zheng, J. L. Sonnenberg, M. Hada, M. Ehara, K. Toyota, R. Fukuda, J. Hasegawa, M. Ishida, T. Nakajima, Y. Honda, O. Kitao, H. Nakai, T. Vreven, J. J. A. Montgomery, J. E. Peralta, F. Ogliaro, M. Bearpark, E. B. J. J. Heyd, K. N. Kudin, V. N. Staroverov, R. Kobayashi, J. Normand, K. Raghavachari, A. Rendell, J. C. Burant, S. S. Iyengar, J. Tomasi, M. Cossi, N. Rega, J. M. Millam, M. Klene, J. E. Knox, J. B. Cross, V. Bakken, C. Adamo, J. Jaramillo, R. Gomperts, R. E. Stratmann, O. Yazyev, A. J. Austin, R. Cammi, C. Pomelli, J. W. Ochterski, R. L. Martin, K. Morokuma, V. G. Zakrzewski, G. A. Voth, P. Salvador, J. J. Dannenberg, S. Dapprich, A. D. Daniels, O. Farkas, J. B. Foresman, J. V. Ortiz, J. Cioslowski and D. J. Fox, *Gaussian 09, Revision D.01*, Gaussian Inc., Wallingford CT, 2009.
- 13 T. J. Wallington, J. M. Andino, I. M. Lorkovic, E. W. Kaiser and G. Marston, *J. Phys. Chem.*, 1990, **94**, 3644–3648.
- 14 R. Atkinson, D. L. Baulch, R. A. Cox, J. N. Crowley, R. F. Hampson, R. G. Hynes, M. E. Jenkin, M. J. Rossi and J. Troe, *Atmos. Chem. Phys.*, 2006, **6**, 3625–4055.
- 15 R. Søndergaard, O. J. Nielsen, M. D. Hurley, T. J. Wallington and R. Singh, *Chem. Phys. Lett.*, 2007, **443**, 199–204.
- 16 M. D. Hurley, J. C. Ball and T. J. Wallington, *J. Phys. Chem. A*, 2007, **111**, 9789–9795.
- 17 M. Mashino, Y. Ninomiya, M. Kawasaki, T. J. Wallington and M. D. Hurley, *J. Phys. Chem. A*, 2000, **104**, 7255–7260.
- 18 L. L. Andersen, F. F. Østerstrøm, M. P. Sulbaek Andersen, O. J. Nielsen and T. J. Wallington, *Chem. Phys. Lett.*, 2015, **639**, 289–293.
- 19 M. P. Sulbaek Andersen, E. J. K. Nilsson, O. J. Nielsen, M. S. Johnson, M. D. Hurley and T. J. Wallington, *J. Photochem. Photobiol., A*, 2008, **199**, 92–97.
- 20 R. J. Meagher, M. E. McIntosh, M. D. Hurley and T. J. Wallington, *Int. J. Chem. Kinet.*, 1997, **29**, 619–625.
- 21 Absorption cross section obtained from Dr T. J. Wallington, Ford Motor Company, private communication July 2016.
- 22 T. J. Wallington, M. D. Hurley, O. J. Nielsen and J. Sehested, *J. Phys. Chem.*, 1994, **98**, 5686–5694.
- 23 B. Ballesteros, E. Jiménez, A. Moreno, A. Soto, M. Antiñolo and J. Albaladejo, *Chemosphere*, 2017, **167**, 330–343.
- 24 Y. Diaz-de-Mera, A. Aranda, A. Notario, A. Rodriguez, D. Rodriguez and I. Bravo, *Phys. Chem. Chem. Phys.*, 2015, **17**, 22991–22998.
- 25 M. P. Sulbaek Andersen, O. J. Nielsen, M. D. Hurley, J. C. Ball, T. J. Wallington, J. E. Stevens, J. W. Martin, D. A. Ellis and S. A. Mabury, *J. Phys. Chem. A*, 2004, **108**, 5189–5196.
- 26 T. J. Wallington and M. D. Hurley, *Int. J. Chem. Kinet.*, 1993, **25**, 819–824.
- 27 J. G. Calvert, J. N. Pitts Jr., *Photochemistry*, John Wiley and Sons Inc., New York, 1966.
- 28 B. J. Finlayson-Pitts, J. N. Pitts Jr., *Kinetics and Atmospheric Chemistry, Chemistry of the Upper and Lower Atmosphere*, Academic Press, San Diego, 2000, ch. 5, pp. 130–178.
- 29 B. J. Finlayson-Pitts, J. N. Pitts Jr., *Rates and Mechanisms of Gas-Phase Reactions in Irradiated Organic-NO_x-Air Mixtures, Chemistry of the Upper and Lower Atmosphere*, Academic Press, San Diego, 2000, ch. 6, pp. 179–263.
- 30 R. Prinn, J. Huang, R. Weiss, D. Cunnold, P. Fraser, P. Simmonds, A. McCulloch, C. Harth, P. Salameh and S. O'Doherty, *Science*, 2001, **292**, 1882–1888.
- 31 W. Allan, H. Struthers, D. C. Lowe and S.E. Mikaloff Fletcher, *J. Geophys. Res.: Atmos.*, 2010, **115**, 8.
- 32 C. M. Spivakovsky, J. A. Logan, S. A. Montzka, Y. J. Balkanski, M. Foreman-Fowler, D. B. A. Jones, L. W. Horowitz, A. C. Fusco, C. A. M. Brenninkmeijer, M. J. Prather, S. C. Wofsy and M. B. McElroy, *J. Geophys. Res.: Atmos.*, 2000, **105**, 8931–8980.
- 33 S. Pinnock, M. D. Hurley, K. P. Shine, T. J. Wallington and T. J. Smyth, *J. Geophys. Res.: Atmos.*, 1995, **100**, 23227–23238.
- 34 Ø. Hodnebrog, M. Etminan, J. S. Fuglestedt, G. Marston, G. Myhre, C. J. Nielsen, K. P. Shine and T. J. Wallington, *Rev. Geophys.*, 2013, **51**, 300–378.
- 35 IPCC, *Climate Change 2013: The Physical Science Basis. Contribution of Working Group I to the Fifth Assessment Report of the Intergovernmental Panel on Climate Change*, Cambridge University Press, Cambridge, United Kingdom and New York, NY, USA, 2013, p. 1535.
- 36 N. R. Greiner, *J. Chem. Phys.*, 1968, **48**, 1413.
- 37 G. Paraskevopoulos and W. S. Nip, *Can. J. Chem.*, 1980, **58**, 2146–2149.
- 38 T. Gierczak, M. Baasandorj and J. B. Burkholder, *J. Phys. Chem. A*, 2014, **118**, 11015–11025.
- 39 V. C. Papadimitriou and J. B. Burkholder, *J. Phys. Chem. A*, 2016, **120**, 6618–6628.

